

ESI for

Palladium(II) complexes bearing 1,2,3-triazole based organosulfur/ selenium ligand: synthesis, structure and applications in Heck and Suzuki-Miyaura coupling as catalyst via palladium nanoparticles

Fariha Saleem, G. K. Rao, Arun Kumar, Satyendra Kumar, Mahabir P. Singh and Ajai K. Singh*

Department of Chemistry, Indian Institute of Technology Delhi, New Delhi-110016, India

E-mail: aksingh@chemistry.iitd.ac.in, ajai57@hotmail.com

Table S1 Crystal data and structural refinements for Complexes 1 / 2

Compounds	1	2
Empirical formula	C₁₆ H₁₅ Cl₂ N₃ Pd S	C₁₆ H₁₅ Cl₂ N₃ Pd Se
Formula wt.	458.68	505.57
Crystal size [mm]	0.34×0.31×0.23	0.48×0.25×0.22
Crystal system	Monoclinic	Orthorhombic
Space group	P2(1)/c	P2(1)2(1)2(1)
Unit Cell dimension	<i>a</i> = 8.482(3) Å <i>b</i> = 11.062(4) Å <i>c</i> = 18.913(7) Å α = 90.00° β = 92.849(6)° γ = 90.00°	<i>a</i> = 8.8269(19) Å <i>b</i> = 9.289(2) Å <i>c</i> = 20.716(4) Å α = 90.00° β = 90.00° γ = 90.00°
Volume [Å ³]	1772.4(11)	1698.6(6)
<i>Z</i>	4	4
ρ_{calcd} [g/cm ³]	1.719	1.977
$\mu(\text{MoK}\alpha)$ [mm ⁻¹]	1.467	3.551
<i>F</i> (000)	912.0	984.0
θ range [°]	2.13–25.00	1.97–24.99
Index ranges	-10 ≤ <i>h</i> ≤ 10 -13 ≤ <i>k</i> ≤ 13 -22 ≤ <i>l</i> ≤ 22	-10 ≤ <i>h</i> ≤ 10 -11 ≤ <i>k</i> ≤ 11 -24 ≤ <i>l</i> ≤ 24
Reflections collected	16478	16232
Independent reflections(<i>R</i> _{int.})	3116 (0.0363)	2998 (0.0477)
Completeness to max. θ [%]	100	100
Max./min. Transmission	0.610 / 0.717	0.072 / 0.036
Data/restraints/ parameters	3116 / 0 / 208	2998 / 0 / 208
Goodness-of-fit on <i>F</i> ²	1.278	1.147
Final <i>R</i> indices [<i>I</i> > 2 σ (<i>I</i>)]	<i>R</i> ₁ = 0.0472, <i>wR</i> ₂ = 0.0943	<i>R</i> ₁ = 0.0355, <i>wR</i> ₂ = 0.0782
<i>R</i> indices (all data)	<i>R</i> ₁ = 0.0507, <i>wR</i> ₂ = 0.0959	<i>R</i> ₁ = 0.0389, <i>wR</i> ₂ = 0.0794
Largest diff. peak/hole[e.Å ⁻³]	0.874 / -0.852	0.979 / -0.483

Table S2 Selected bond lengths [\AA] and bond angles [$^\circ$]

Compounds	Bond length [\AA]		Bond angle [$^\circ$]	
1	N(3)—Pd(1)	2.005(4)	N(3)—Pd(1)—Cl(1)	174.04(11)
	Pd(1)—S(1)	2.2727(14)	N(3)—Pd(1)—Cl(2)	92.72(11)
	Cl(1)—Pd(1)	2.2968(14)	S(1)—Pd(1)—Cl(1)	89.01(5)
	Cl(2)—Pd(1)	2.3003(13)	S(1)—Pd(1)—Cl(2)	177.91(5)
	N(2)—N(3)	1.312(5)	Cl(1)—Pd(1)—Cl(2)	93.09(5)
	C(10)—S(1)	1.826(5)	N(3)—Pd(1)—S(1)	85.18(11)
	C(11)—S(1)	1.786(5)	C(11)—S(1)—C(10)	102.3(3)
	C(9)—N(3)	1.368(6)	C(11)—S(1)—Pd(1)	107.07(17)
			C(10)—S(1)—Pd(1)	99.45(17)
2	Pd(1)—N(3)	2.005(4)	N(3)—Pd(1)—Cl(1)	173.41(14)
	Pd(1)—Cl(1)	2.2799(15)	N(3)—Pd(1)—Cl(2)	95.32(14)
	Pd(1)—Cl(2)	2.3146(16)	Cl(1)—Pd(1)—Cl(2)	91.22(6)
	Pd(1)—Se(1)	2.3693(8)	N(3)—Pd(1)—Se(1)	85.37(13)
	Se(1)—C(10)	1.985(6)	Cl(1)—Pd(1)—Se(1)	88.11(4)
	C(11)—Se(1)	1.942(6)	Cl(2)—Pd(1)—Se(1)	178.20(5)
	N(2)—N(3)	1.326(6)	C(11)—Se(1)—C(10)	98.9(3)
	N(3)—C(9)	1.373(7)	C(11)—Se(1)—Pd(1)	104.41(17)
			C(10)—Se(1)—Pd(1)	96.77(19)

Table S3 Non-covalent interactions C—H \cdots Cl distances [\AA] of **1** / **2**

1		2	
C(10)—H(10A) \cdots Cl(1)	2.815(2)	C(18)—H(18) \cdots Cl(2)	3.026(2)
C(10)—H(10B) \cdots Cl(1)	3.033(2)	C(16)—H(16) \cdots Cl(2)	3.122(2)
C(12)—H(12) \cdots Cl(2)	2.822(2)	C(10)—H(10A) \cdots Cl(1)	3.328(2)
C(8)—H(8) \cdots Cl(1)	2.883(5)	C(8)—H(8) \cdots Cl(2)	3.051(2)
C(8)—H(8) \cdots Cl(2)	2.635(3)	C(8)—H(8) \cdots Cl(1)	2.790(2)
C(7)—H(7A) \cdots Cl(1)	2.789(2)	C(7)—H(7A) \cdots Cl(2)	2.959(2)
C(7)—H(7B) \cdots Cl(2)	2.932(2)	C(6)—H(6) \cdots Cl(1)	3.150(2)
		C(4)—H(4) \cdots Cl(1)	3.059(2)

Table S4 Selected bond lengths (Å) and angles (°) for **1** / **2** and the values calculated from DFT studies

1			2		
Bond length / angle			Bond length / angle		
N(3)—Pd(1)	2.005(4)	2.100	N(3)—Pd(1)	2.005(4)	2.099
S(1)—Pd(1)	2.2727(14)	2.513	Se(1)—Pd(1)	2.3693(8)	2.566
Cl(1)—Pd(1)	2.2968(14)	2.371	Cl(1)—Pd(1)	2.2799(15)	2.328
Cl(2)—Pd(1)	2.3003(13)	2.314	Cl(2)—Pd(1)	2.3146(16)	2.325
S(1)—C(10)	1.826(5)	1.908	Se(1)—C(10)	1.985(6)	2.040
S(1)—C(11)	1.786(5)	1.855	Se(1)—C(11)	1.942(6)	1.971
S(1)—Pd—Cl(1)	177.91(5)	175.35	Se(1)—Pd—Cl(1)	178.20(5)	175.44
N3—Pd—Cl(2)	174.04(11)	173.89	N3—Pd—Cl(2)	173.41(14)	174.76
N3—Pd—Cl(1)	92.72(11)	93.39	N3—Pd—Cl(1)	95.32(14)	93.39
S(1)—Pd—N(3)	85.18(11)	82.59	Se(1)—Pd—N(3)	85.37(13)	82.90
Cl(2)—Pd—Cl(1)	93.09(5)	92.58	Cl(2)—Pd—Cl(1)	91.22(6)	92.30
S(1)—Pd—Cl(2)	89.01(5)	91.50	Se(1)—Pd—Cl(2)	88.11(4)	92.02

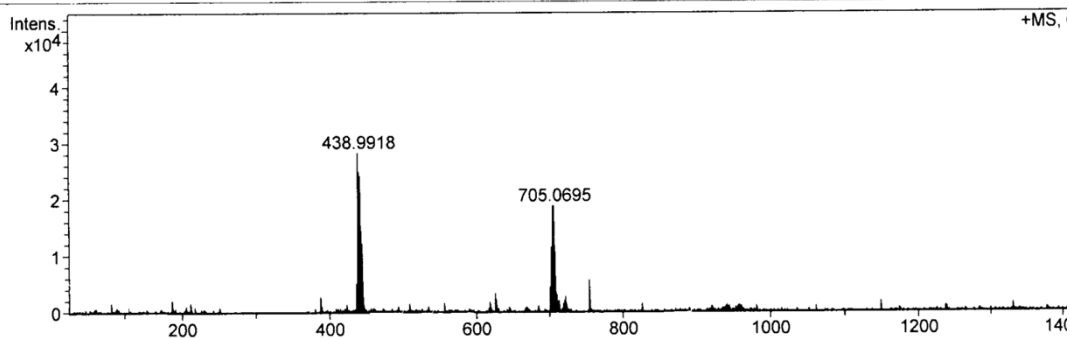
Table S5 HOMO-LUMO energy gap of the **1** / **2** Mulliken partial atomic charge

Complex	Mulliken partial atomic charge						
	Energygap (kcal/mol)	Metal	Calcogen	N of triazole			Cl
				N3	N2	N1	
1	78.5641	-0.038	0.465	-0.326	0.007	-0.196	-0.262
2	78.8025	-0.060	0.520	-0.330	0.015	-0.196	-0.279

Mass Spectrum SmartFormula Report

Analysis Info		Acquisition Date	6/25/2012 10:14:22
Analysis Name	D:\Data\June_12\FAR-1A.d	Operator	Sharma/Singh
Method	tune_low.m	Instrument / Ser#	micrOTOF-Q II 10:
Sample Name			
Comment			

Acquisition Parameter					
Source Type	ESI	Ion Polarity	Positive	Set Nebulizer	0.3 Bar
Focus	Not active	Set Capillary	4500 V	Set Dry Heater	180 °C
Scan Begin	50 m/z	Set End Plate Offset	-500 V	Set Dry Gas	4.0 l/min
Scan End	1500 m/z	Set Collision Cell RF	100.0 Vpp	Set Divert Valve	Source



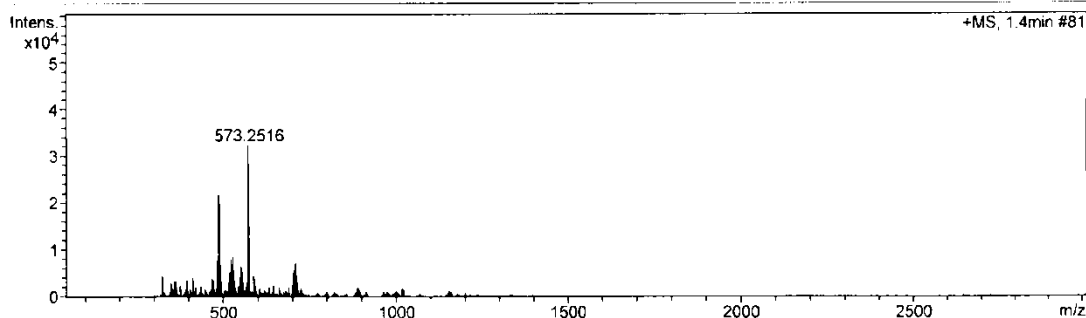
Meas. m/z	#	Formula	Score	m/z	err [mDa]	err [ppm]	mSig	rdb	e ⁻ Conf
479.9304	1	C ₁₆ H ₁₅ Cl ₂ N ₃ NaPdS	100.00	479.9291	-1.3	-2.7	47.1	9.5	even

Fig. S1 Mass spectrum of 1

Mass Spectrum SmartFormula Report

Analysis Info		Acquisition Date	2/22/2012 4:18:34 PM
Analysis Name	D:\Data\FEB_2012\F-3A.d	Operator	Sharma/Singh
Method	tune_wide.m	Instrument / Ser#	micrOTOF-Q II 10262
Sample Name			
Comment			

Acquisition Parameter					
Source Type	ESI	Ion Polarity	Positive	Set Nebulizer	0.3 Bar
Focus	Active	Set Capillary	4500 V	Set Dry Heater	180 °C
Scan Begin	50 m/z	Set End Plate Offset	-500 V	Set Dry Gas	4.0 l/min
Scan End	3000 m/z	Set Collision Cell RF	800.0 Vpp	Set Divert Valve	Source



Meas. m/z	#	Formula	m/z	err [p]	Me an [p]	rd b	N- ul e	e ⁻ Conf	mSi gm a	Std l	St d l m/ z	St Va rN or m/ z	St d m/ z	Std Com b Dev
527.8730	1	C ₁₆ H ₁₅ Cl ₂ N ₃ NaPdSe	527.8738	1.4	0.9	9.5	ok	even	51.8	38.4	1.8	7.8	2.1	842.7

Fig. S2 Mass spectrum of 2

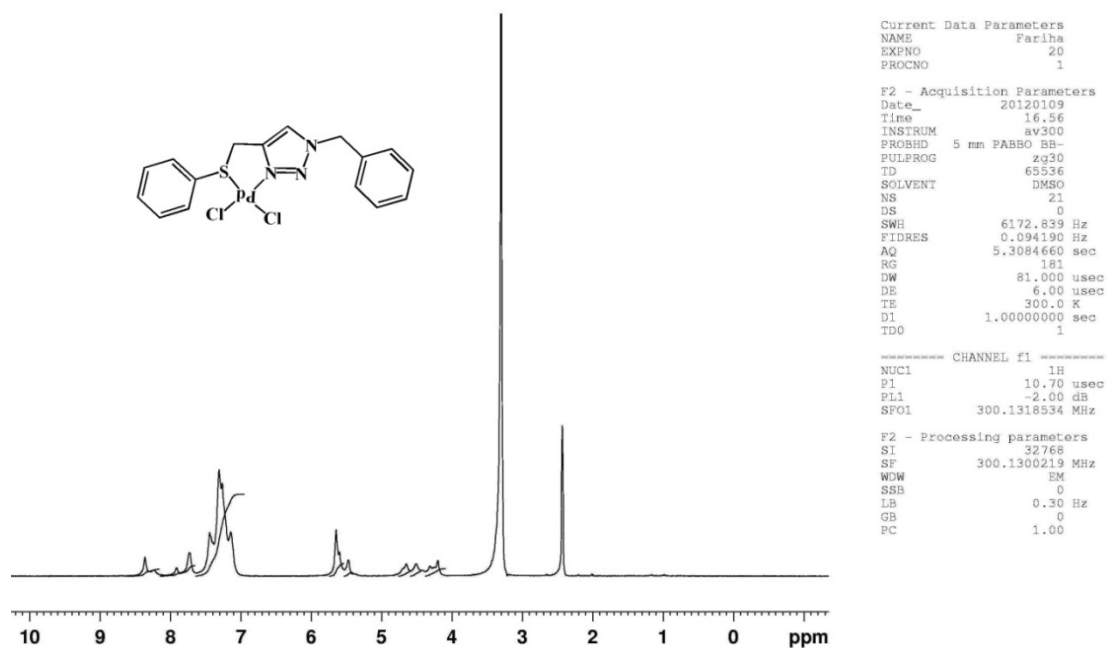


Fig. S3 ^1H NMR spectrum of **1**

fariha Ph-S-Click Pd Complex

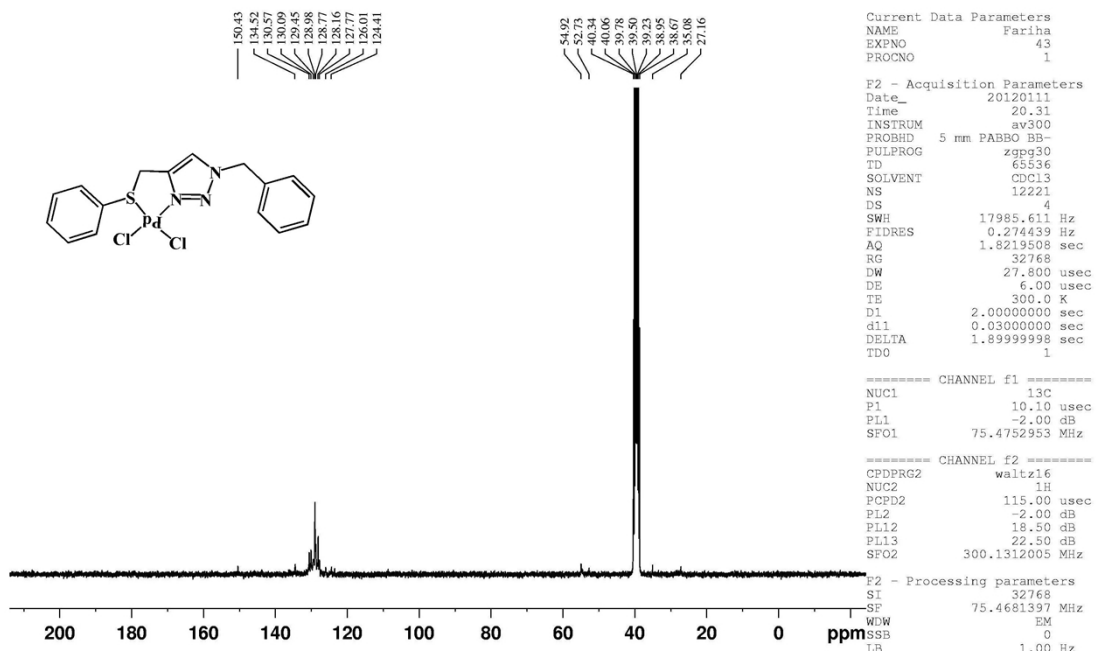


Fig. S4 $^{13}\text{C}\{^1\text{H}\}$ NMR spectrum of **1**

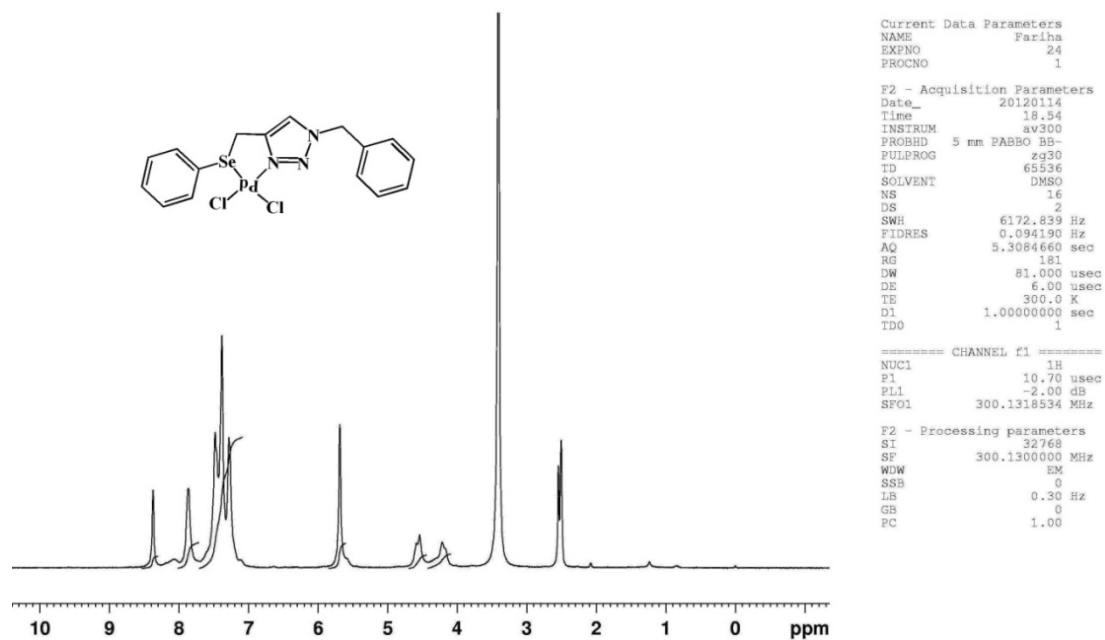


Fig. S5 ^1H NMR spectrum of 2

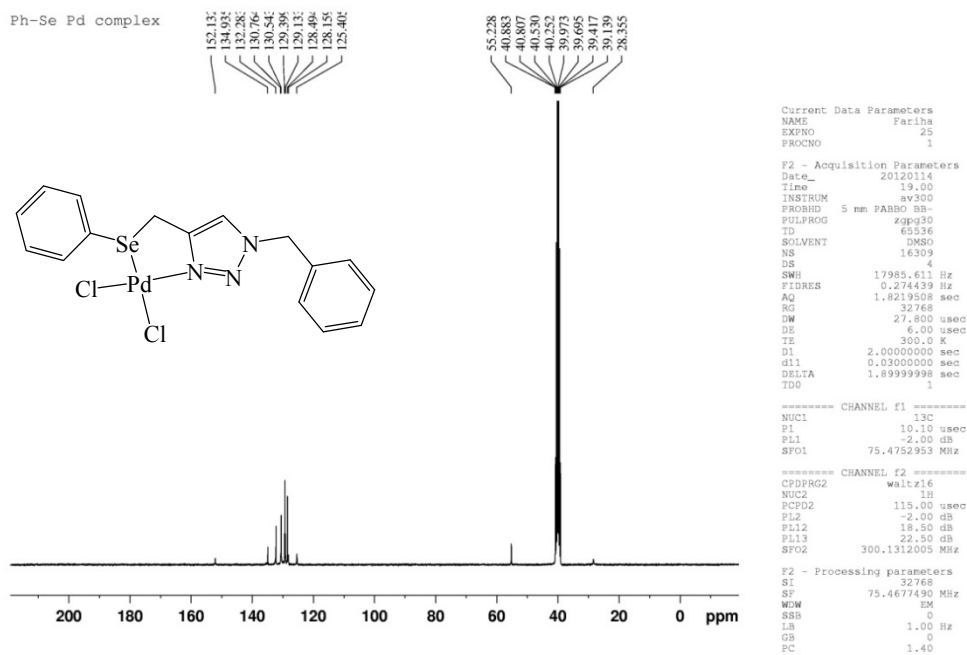


Fig. S6 $^{13}\text{C}\{^1\text{H}\}$ NMR spectrum of 2

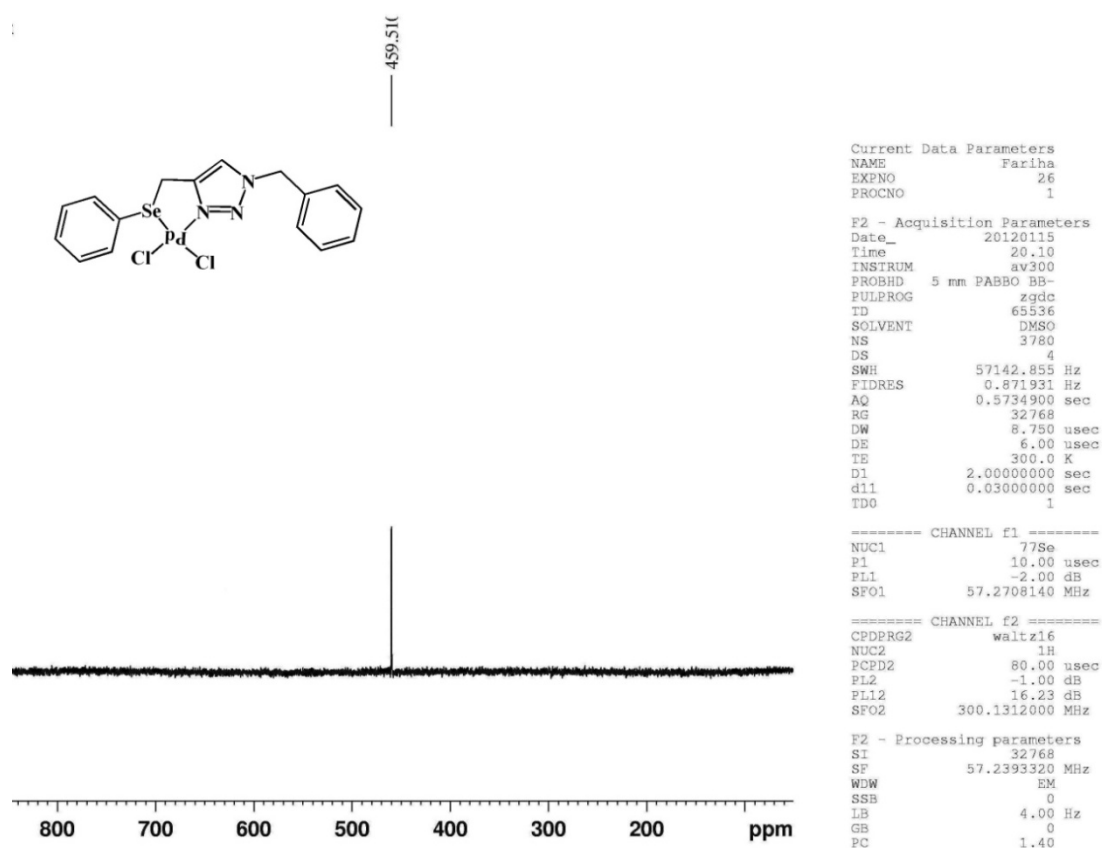


Fig. S7 $^{77}\text{Se}\{^1\text{H}\}$ NMR spectrum of **2**

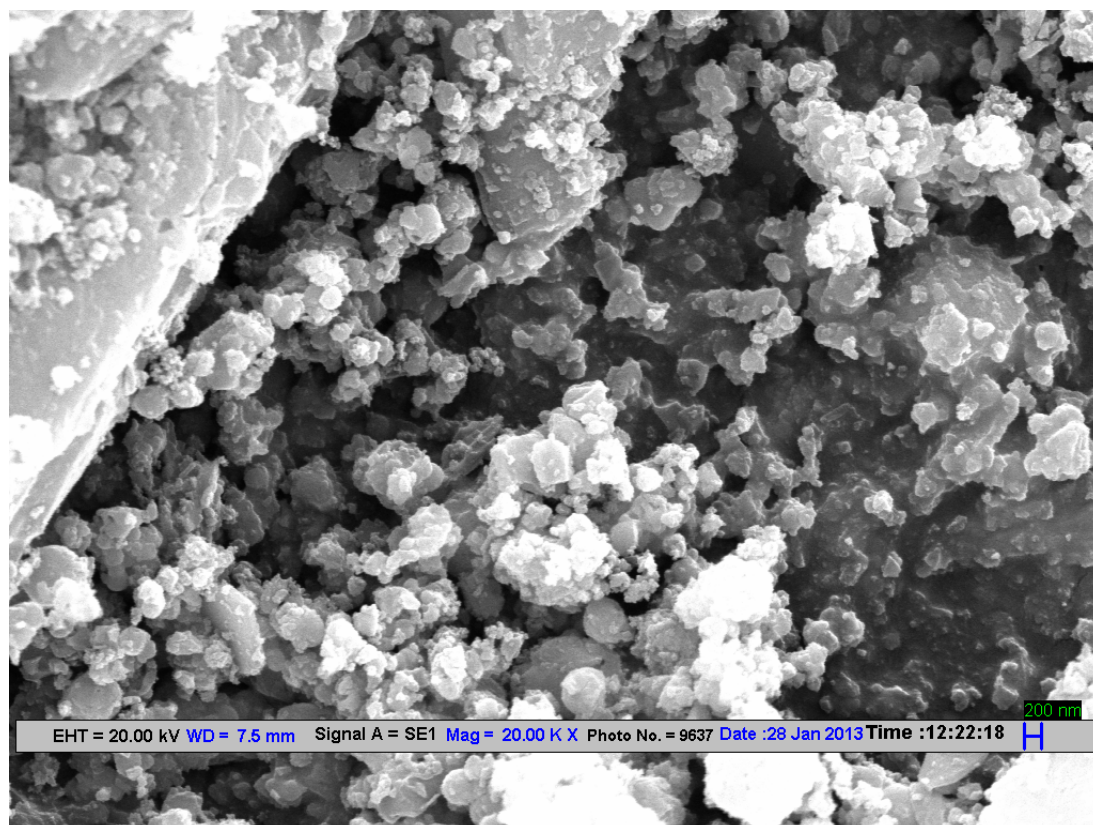


Fig. S8 SEM image of NPs obtained from **1** during Suzuki-Miyaura reaction

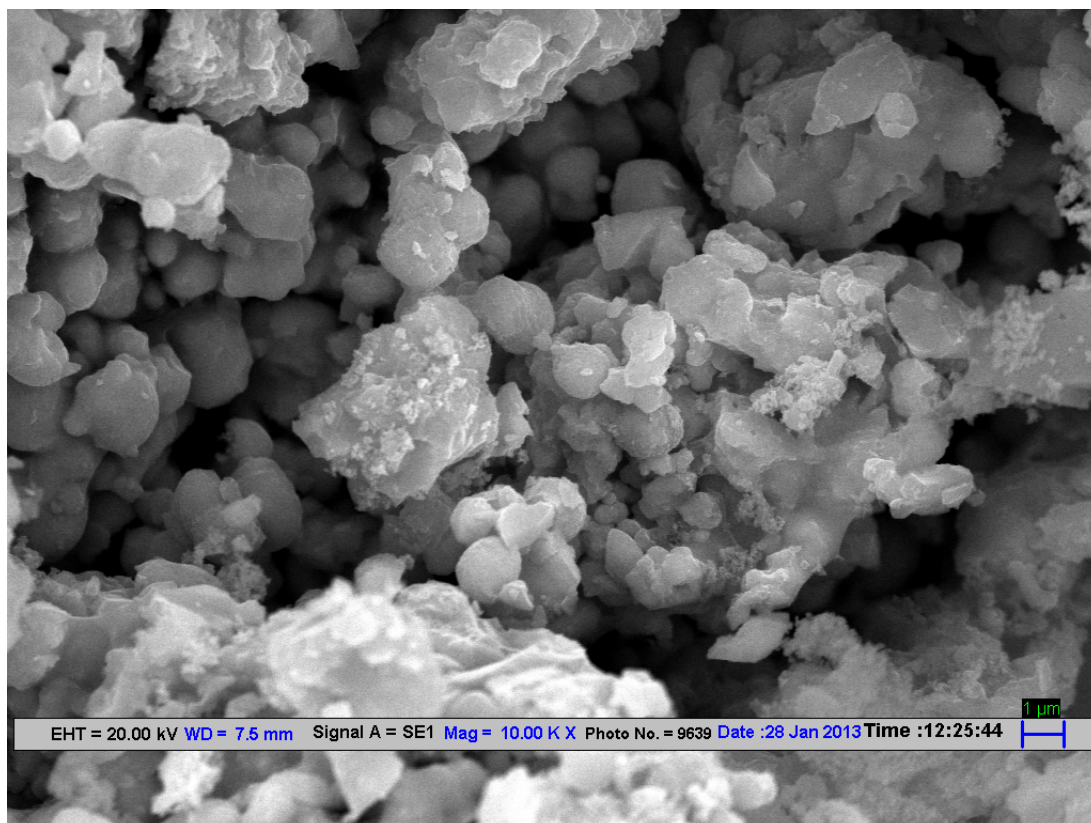


Fig. S9 SEM image of NPs obtained from **2** during Suzuki-Miyaura reaction

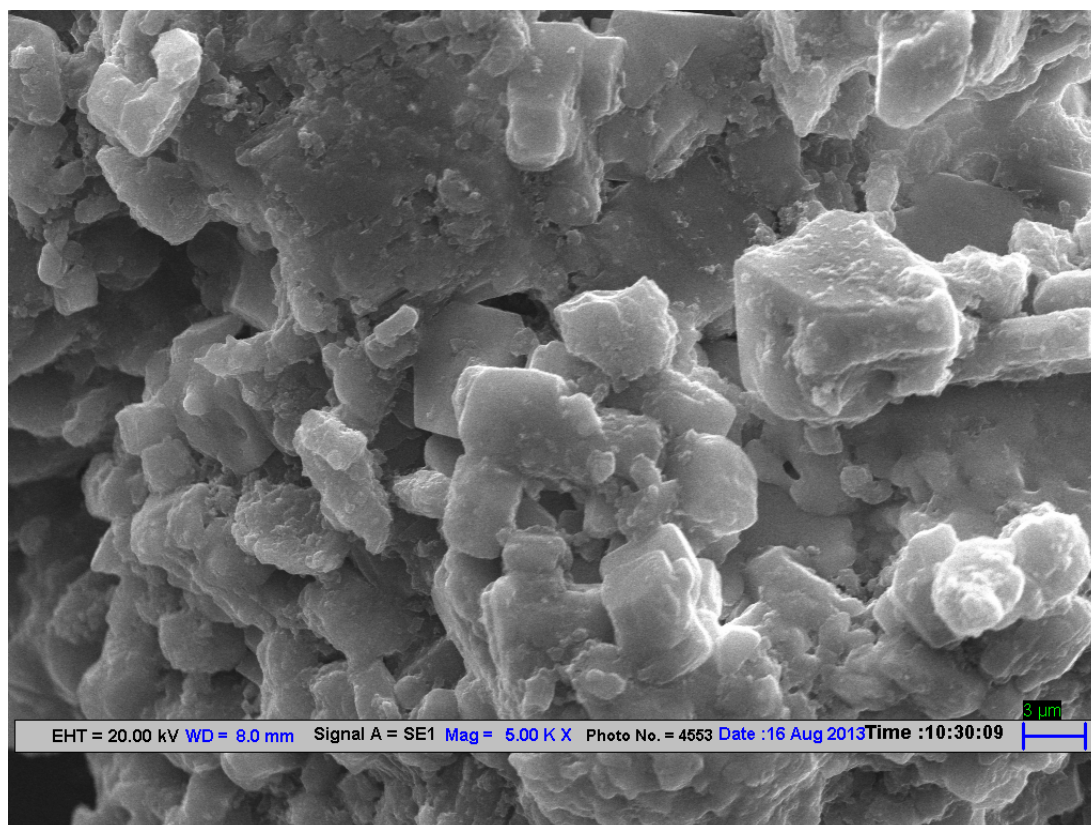


Fig. S10 SEM image of NPs obtained from **1** during Heck reaction

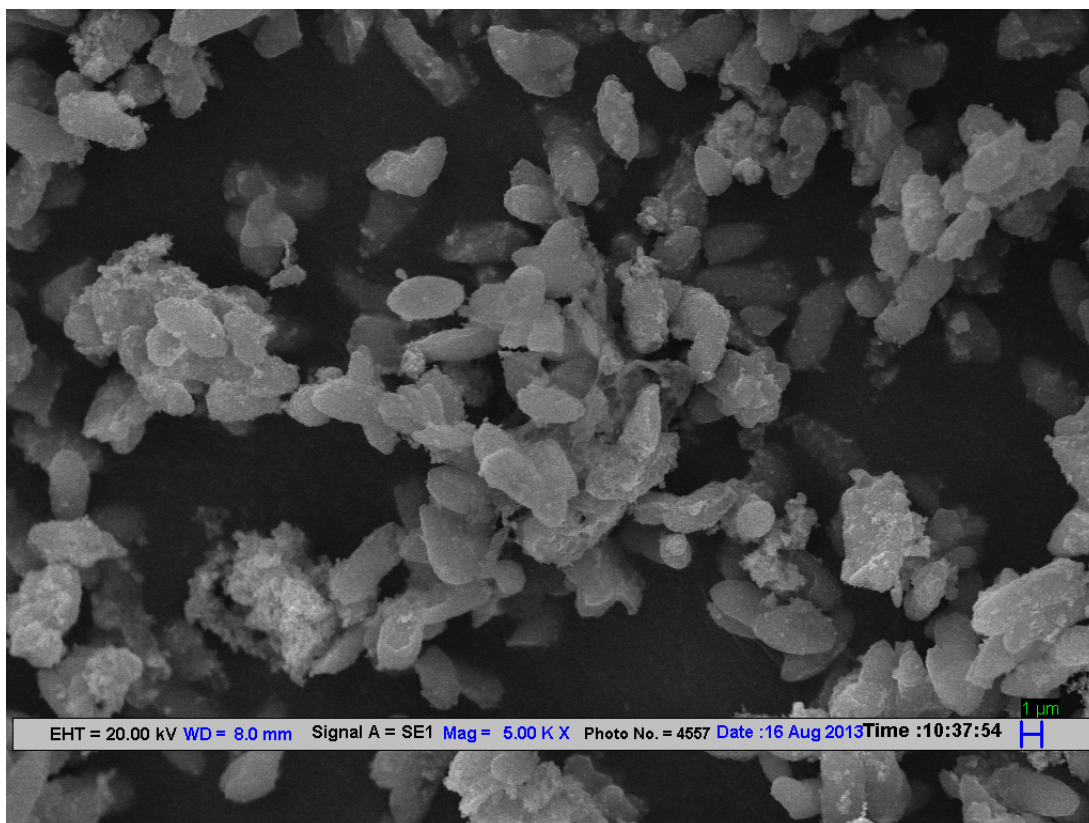
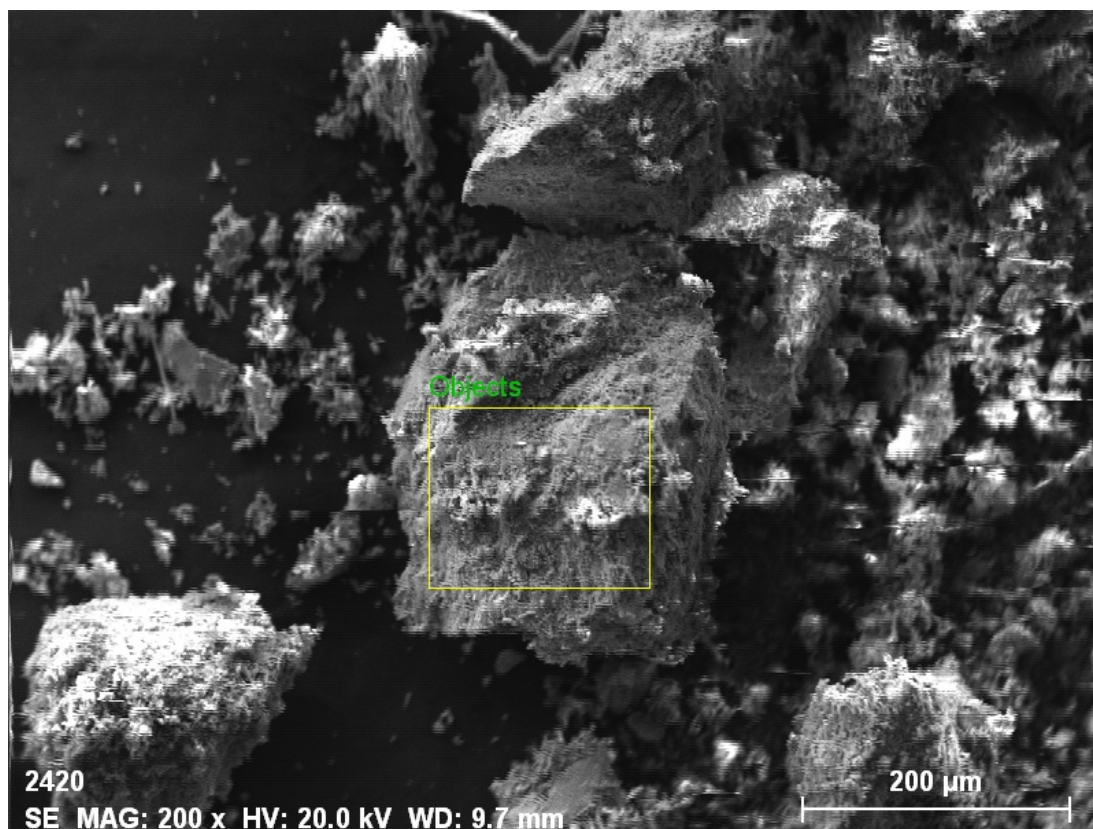


Fig. S11 SEM image of NPs obtained from **2** during Heck reaction



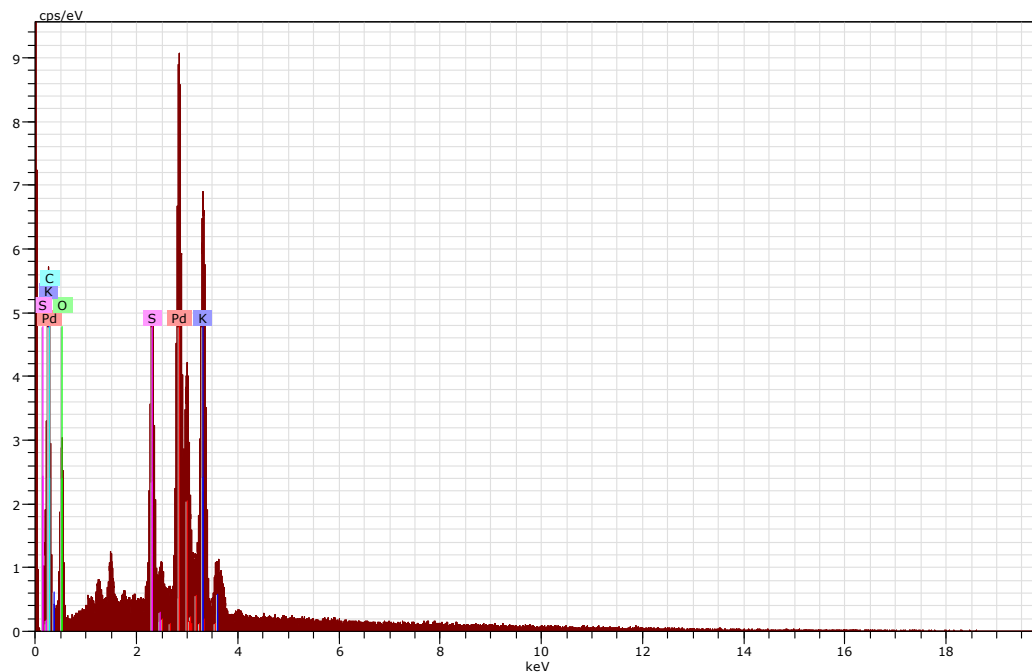
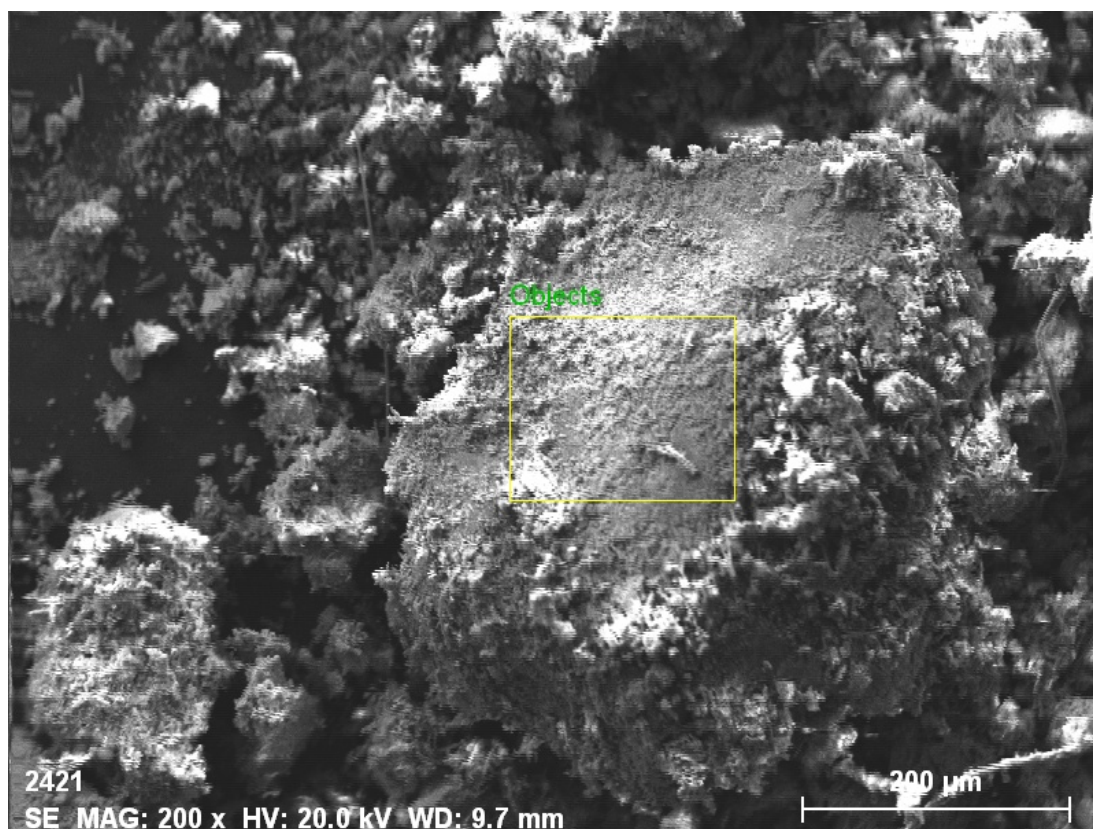


Fig. S12 SEM-EDX image NPs obtained from **1** during Suzuki-Miyaura reaction



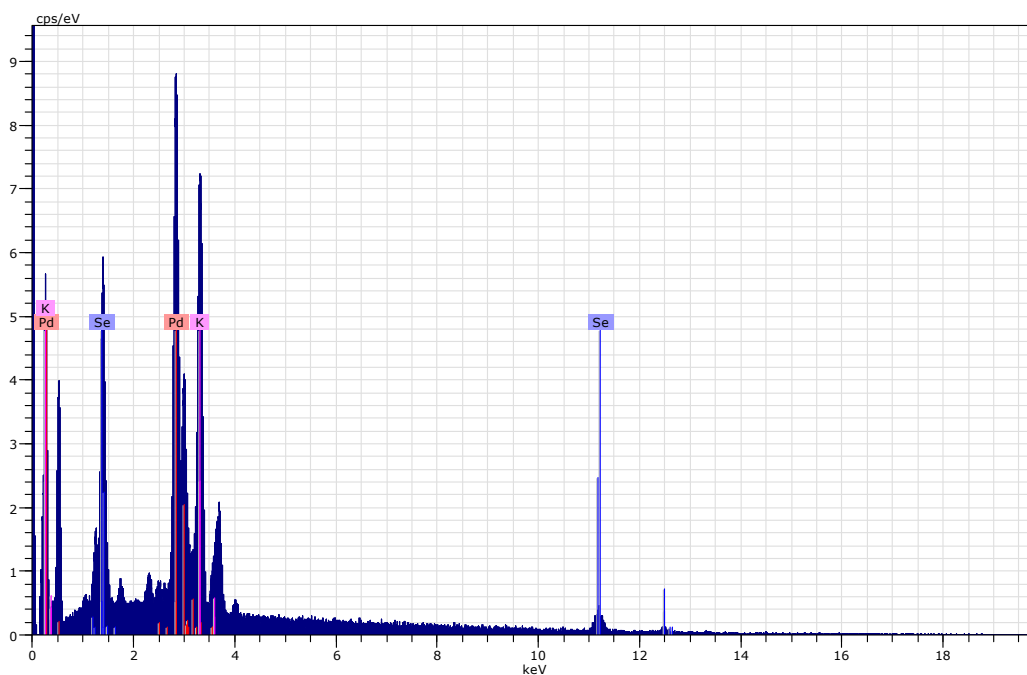
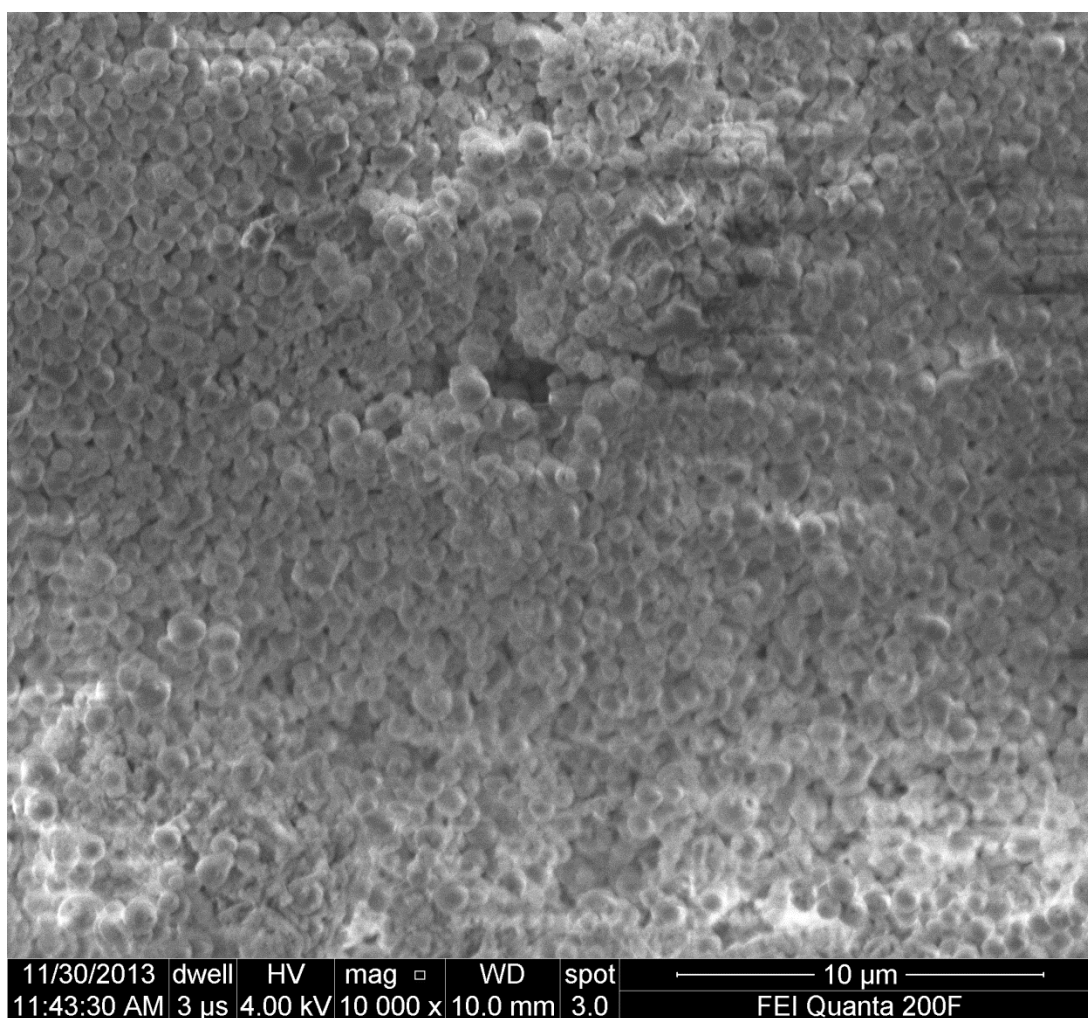


Fig. S13 SEM-EDX image NPs obtained from **2** during Suzuki-Miyaura reaction



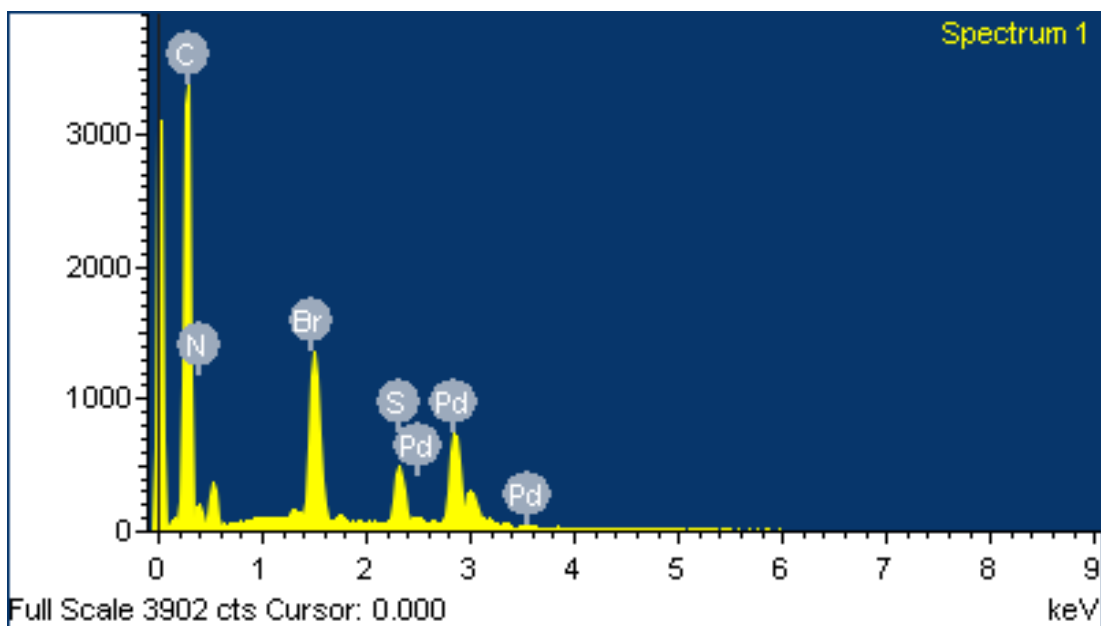
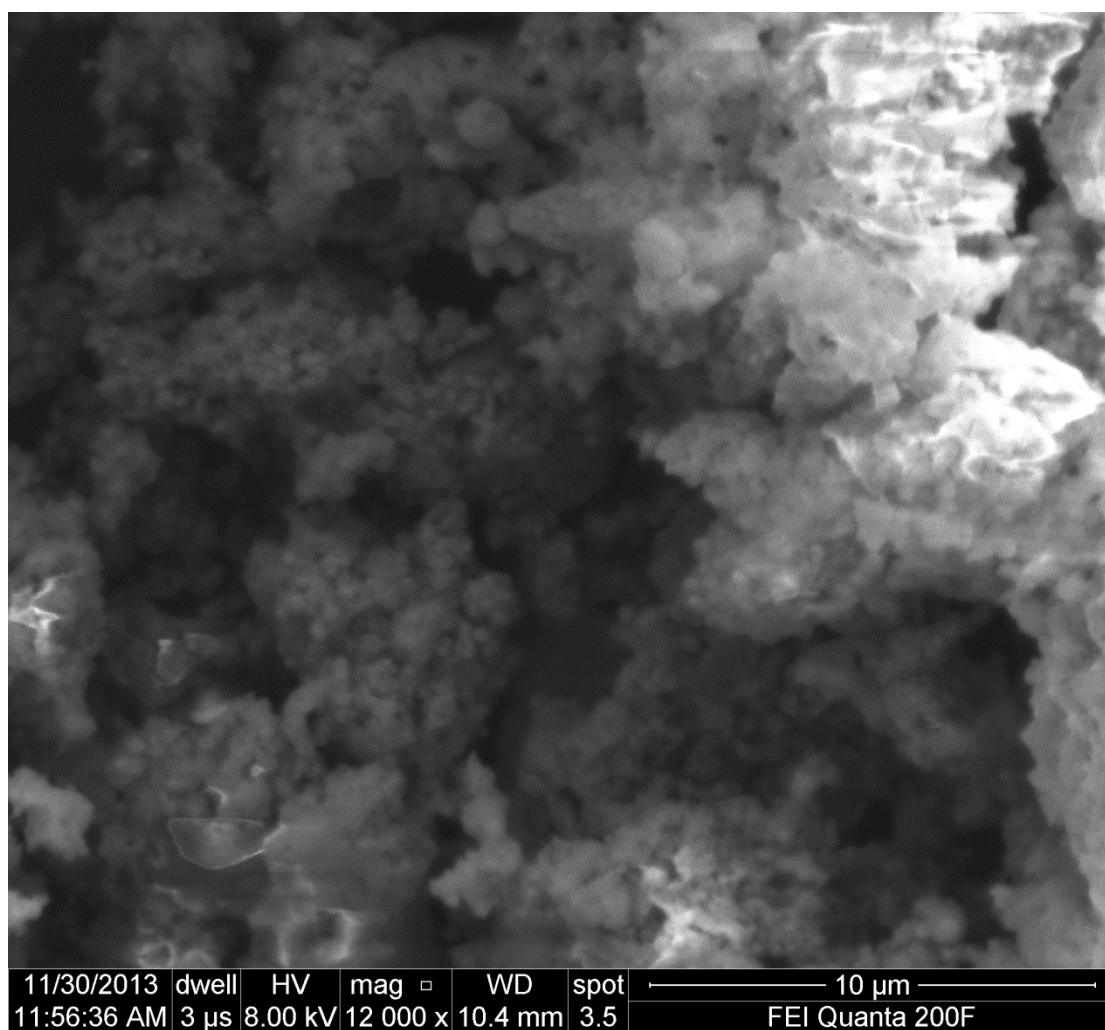


Fig. S14 SEM-EDX image NPs obtained from **1** during Heck reaction



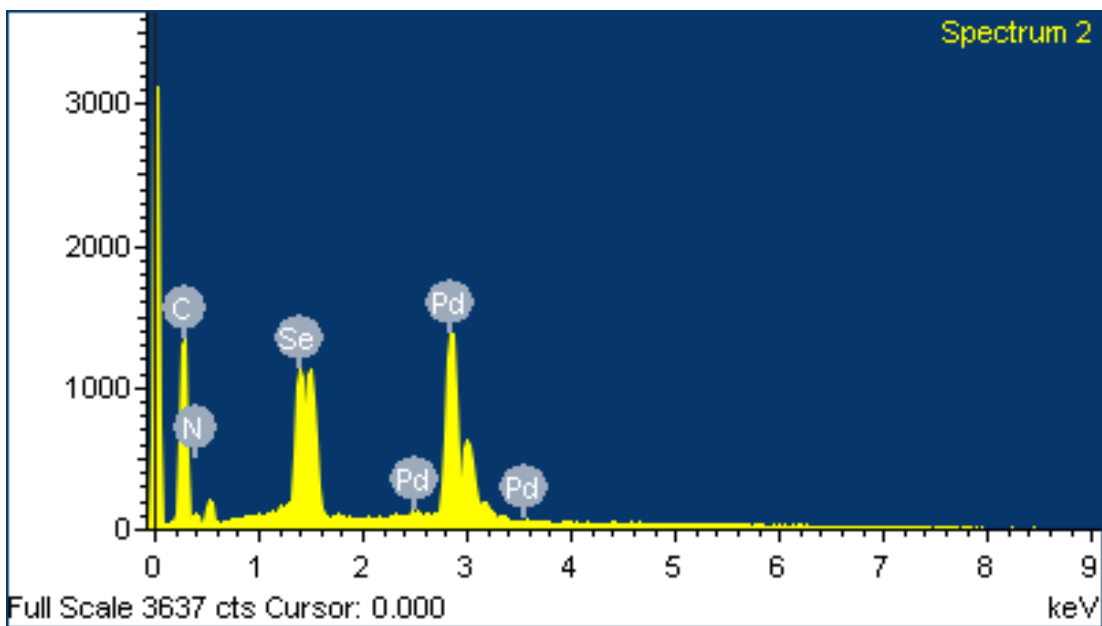


Fig. S15 SEM-EDX image NPs obtained from 2 during Heck reaction

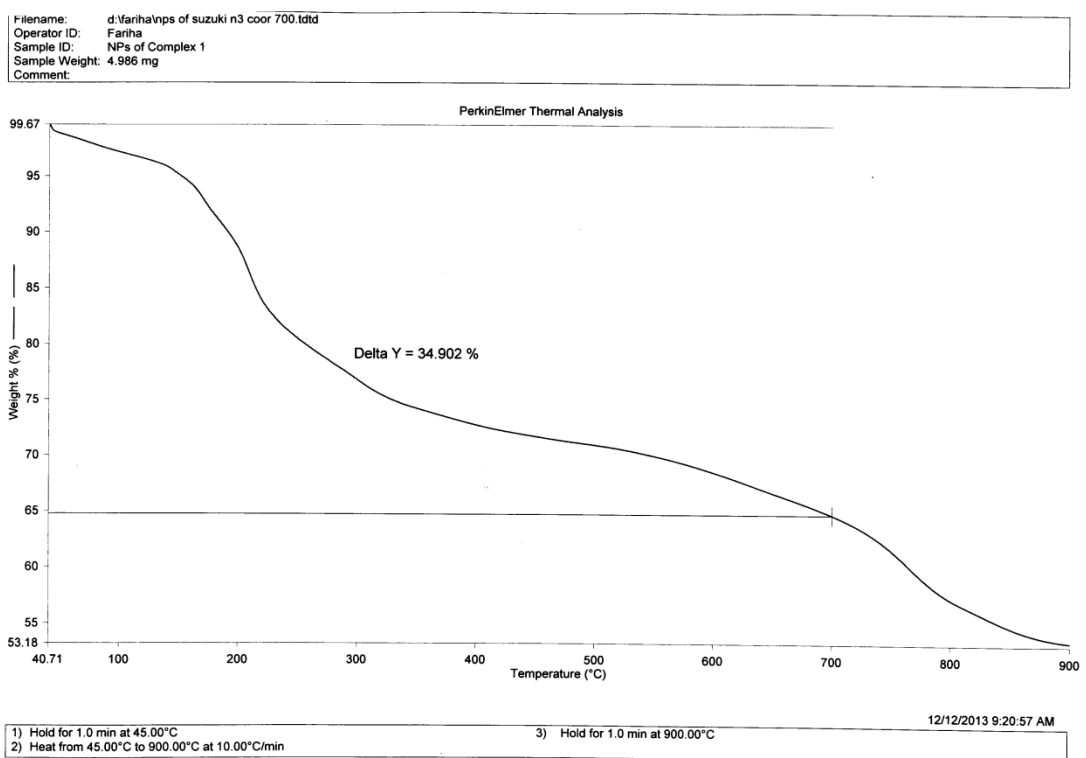
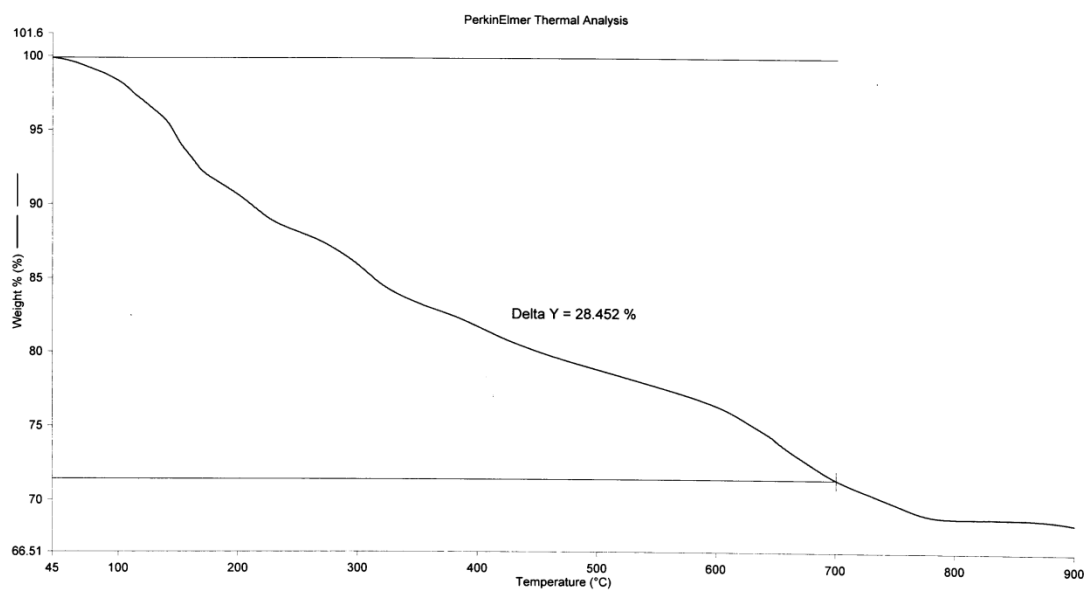


Fig. S16 TGA of NPs obtained from 1 during Suzuki-Miyaura reaction

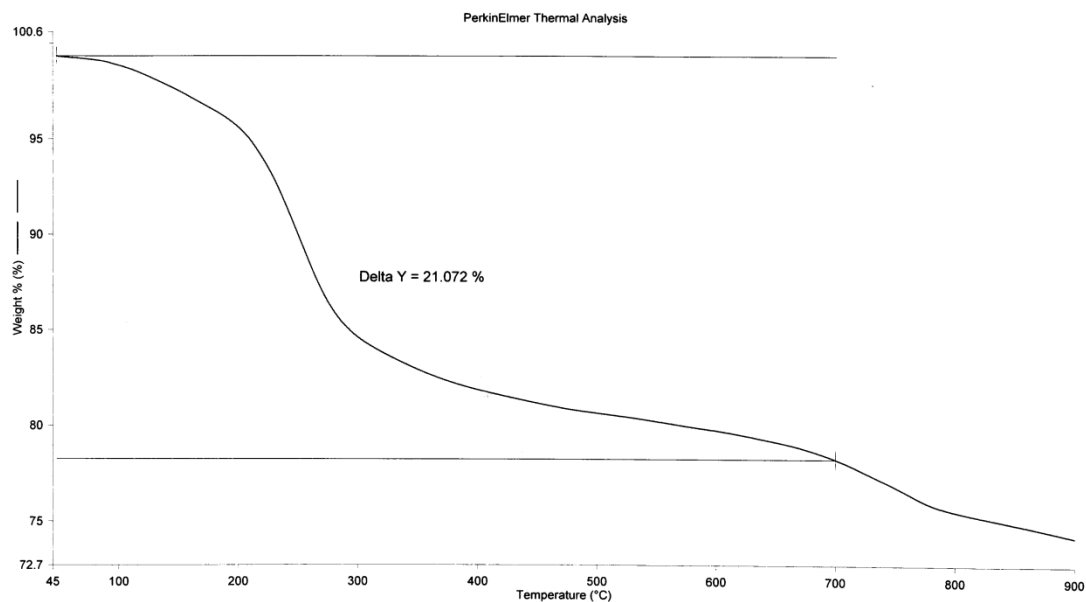
Filename: D:\Fariha...nps of 2 suzuki n3 coor 700.ttdt
Operator ID: Fariha
Sample ID: NPs of Complex 2
Sample Weight: 3.092 mg
Comment:



1) Hold for 1.0 min at 45.00°C
2) Heat from 45.00°C to 900.00°C at 10.00°C/min
3) Hold for 1.0 min at 900.00°C
12/12/2013 9:34:04 AM

Fig. S17 TGA of NPs obtained from **2** during Suzuki-Miyaura reaction

Filename: d:\Fariha...Fariha nps of heck pd-s 700.ttdt
Operator ID: fariha
Sample ID: fariha Nps of Heck Pd-S
Sample Weight: 3.406 mg
Comment:



1) Heat from 45.00°C to 900.00°C at 10.00°C/min
2) Hold for 1.0 min at 900.00°C
12/12/2013 9:27:53 AM

Fig. S18 TGA of NPs obtained from **1** during Heck reaction

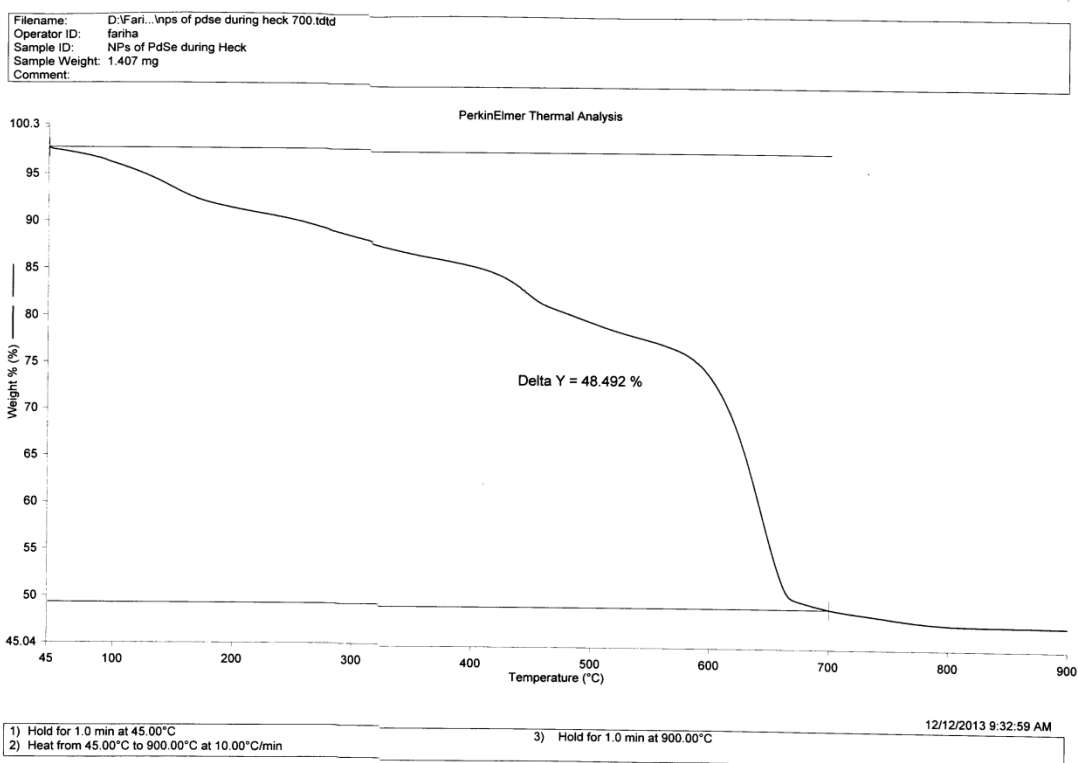


Fig. S19 TGA of NPs obtained from **2** during Heck reaction

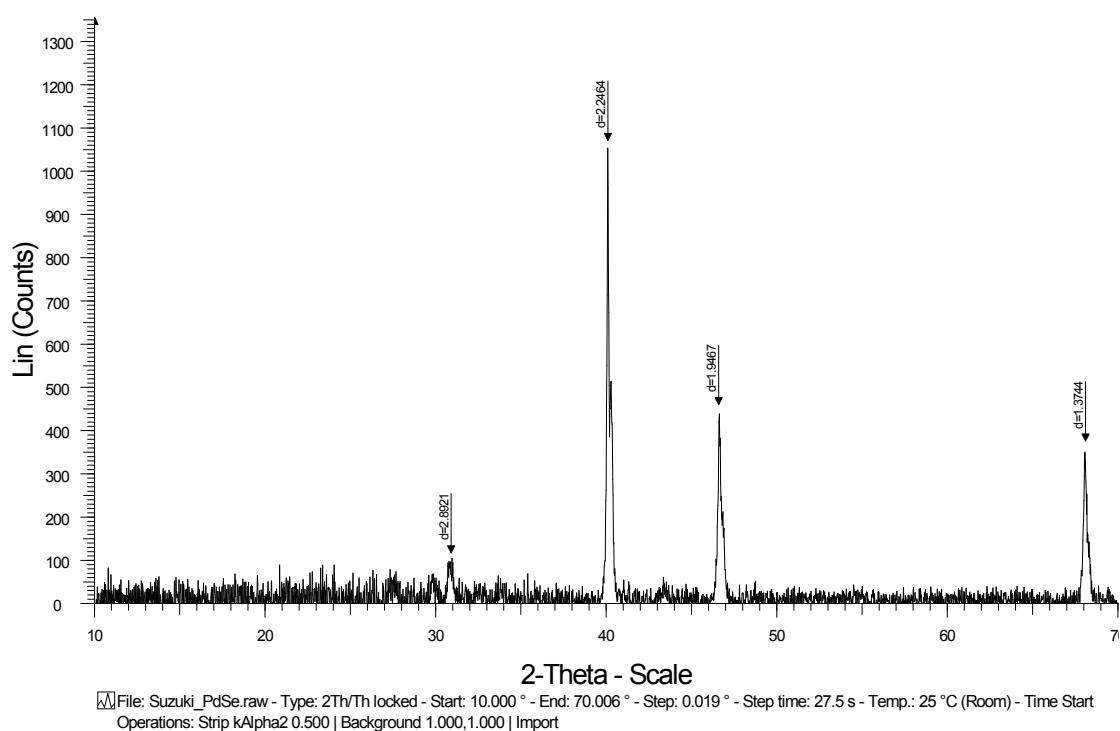


Fig. S20 PXRD of NPs after annealing obtained from **1** during Suzuki-Miyaura reaction

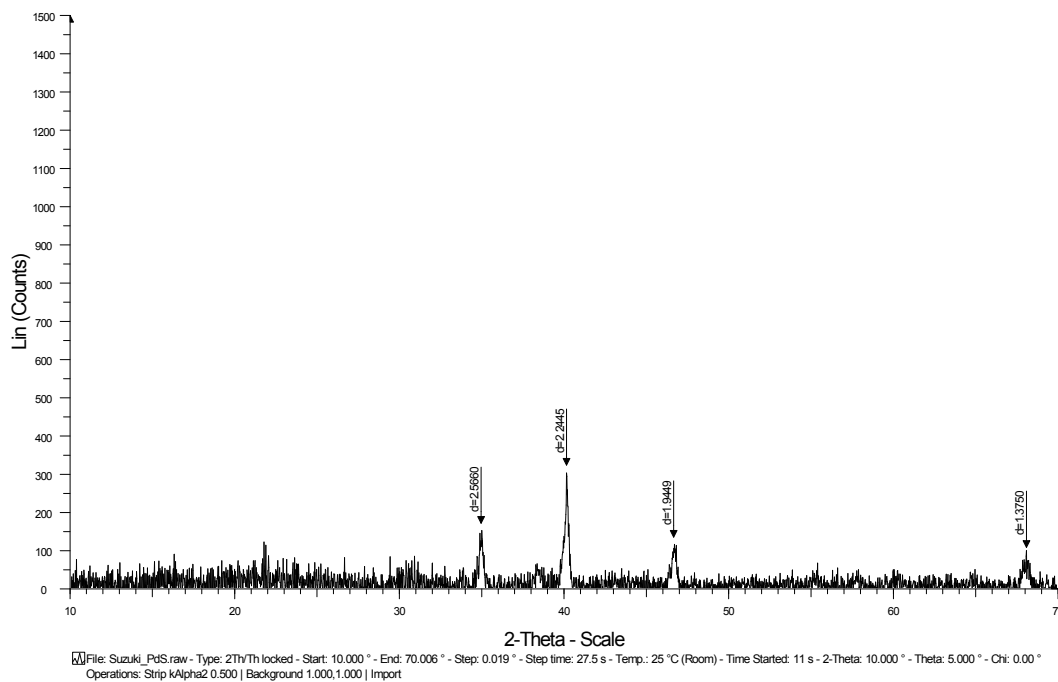


Fig.S21 PXR D of NPs after annealing obtained from **2** during Suzuki-Miyaura reaction

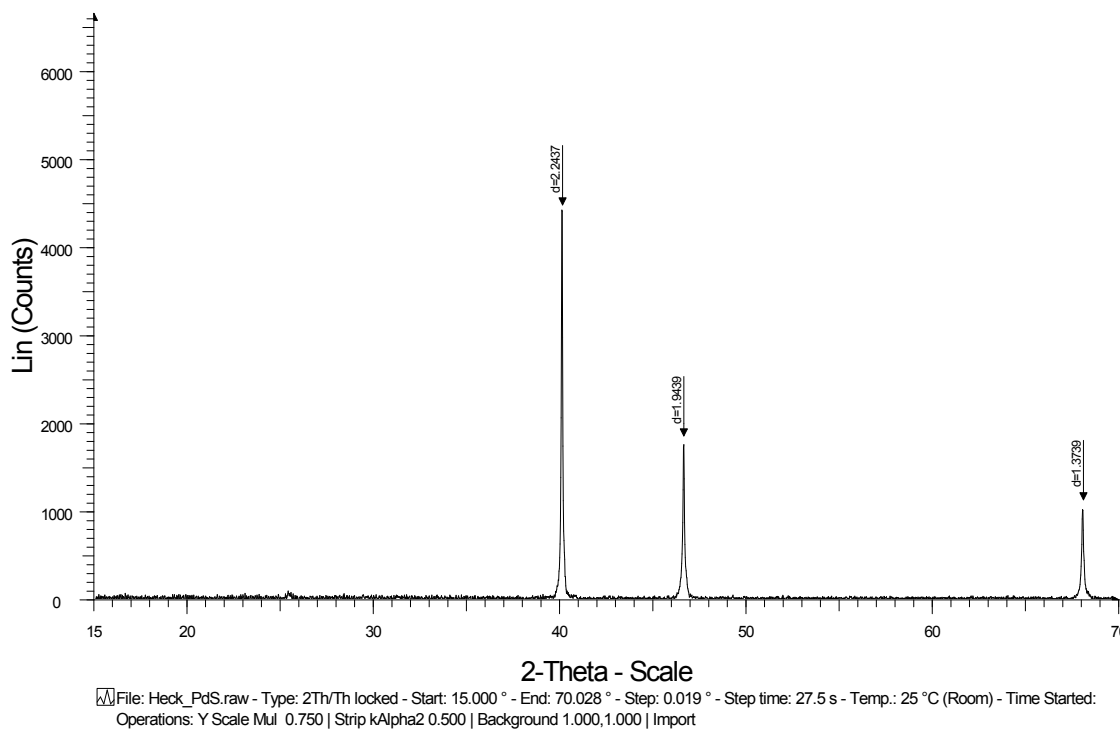


Fig. S22 PXR D of NPs after annealing obtained from **1** during Heck reaction

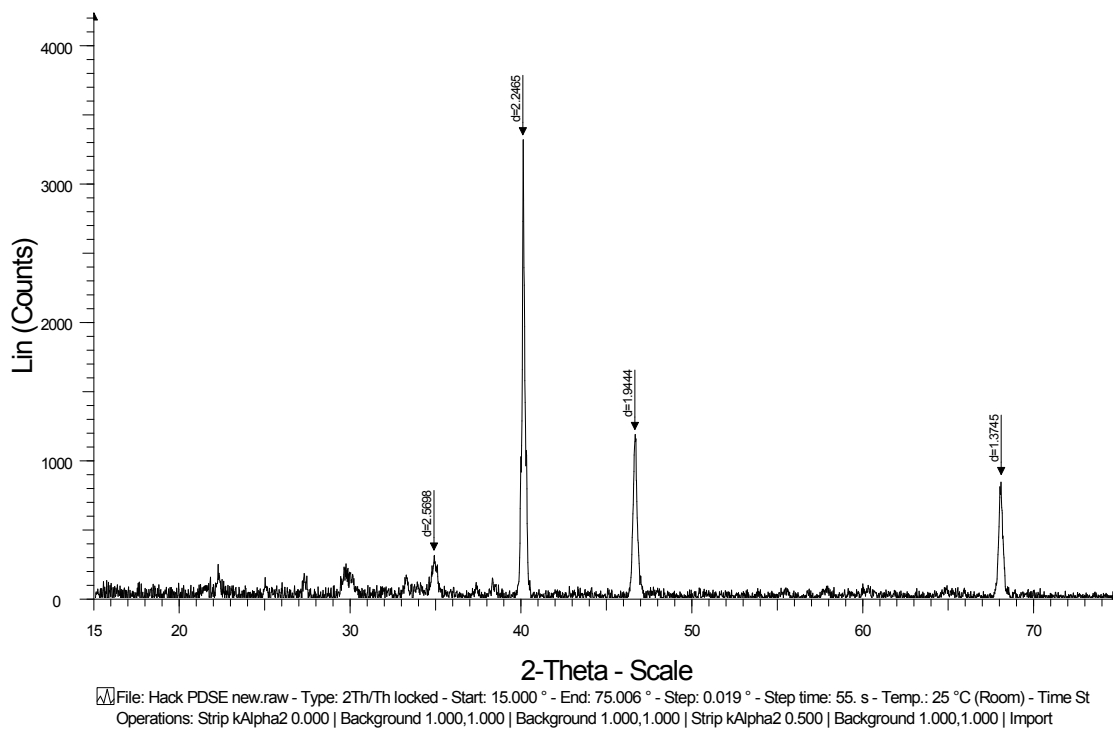


Fig. S23 PXRD of NPs after annealing obtained from **2** during Heck reaction

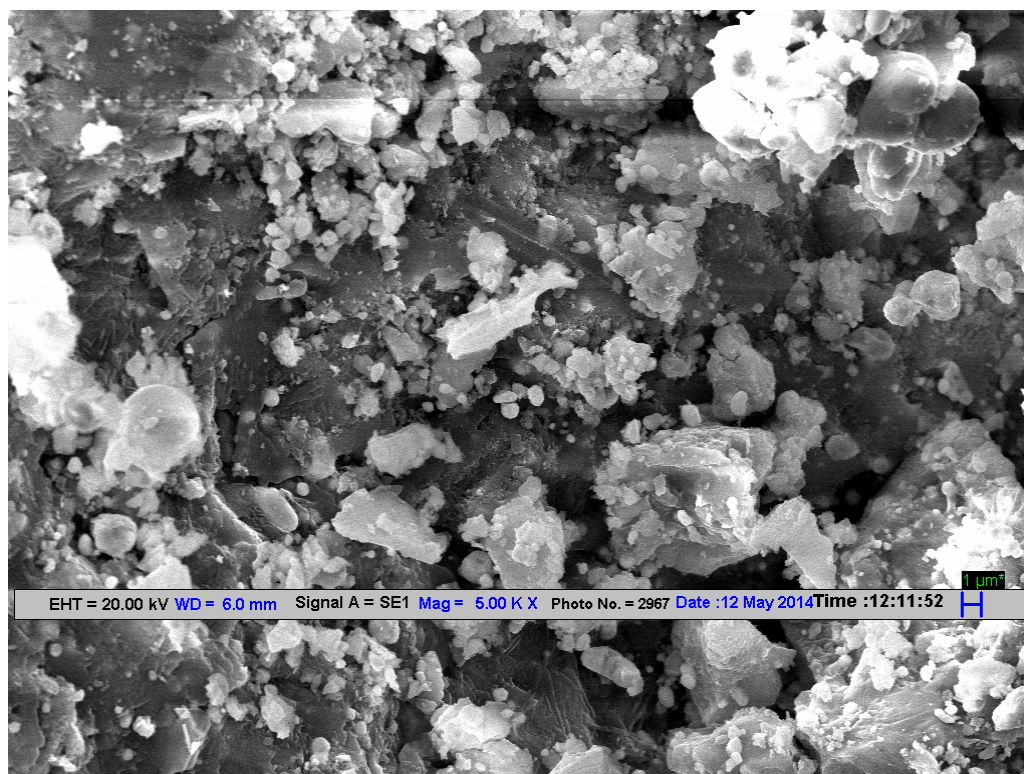


Fig. S24 SEM image of NPs after annealing obtained from **1** during Suzuki-Miyaura reaction

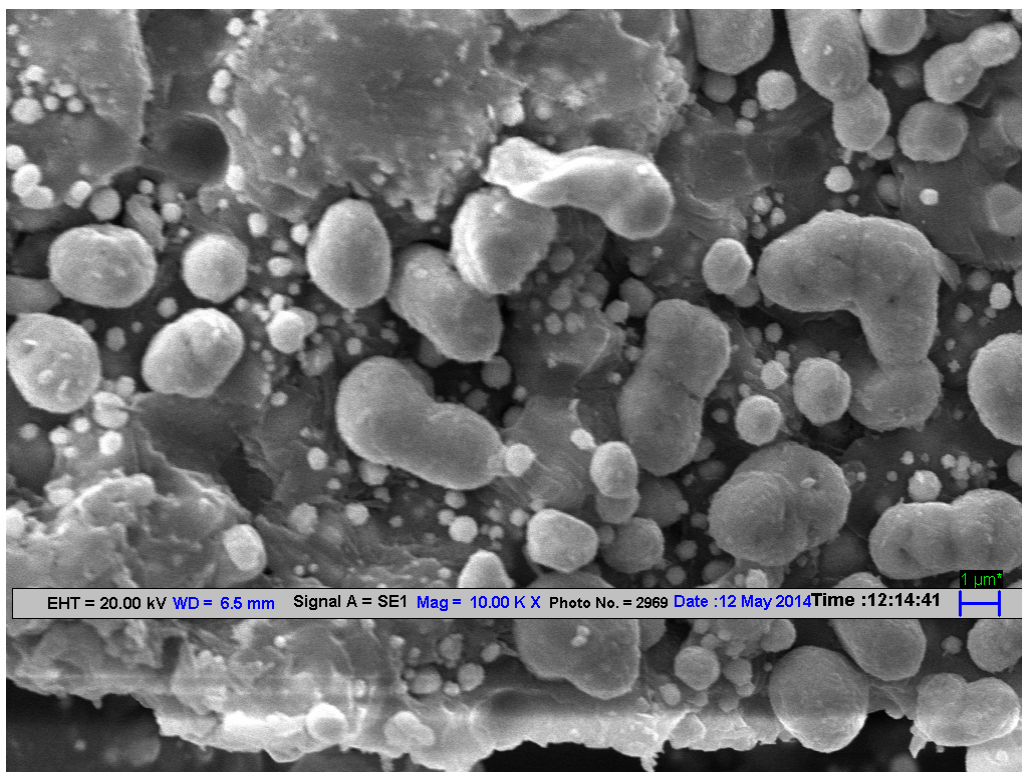


Fig. S25 SEM image of NPs after annealing obtained from **2** during Suzuki-Miyaura reaction

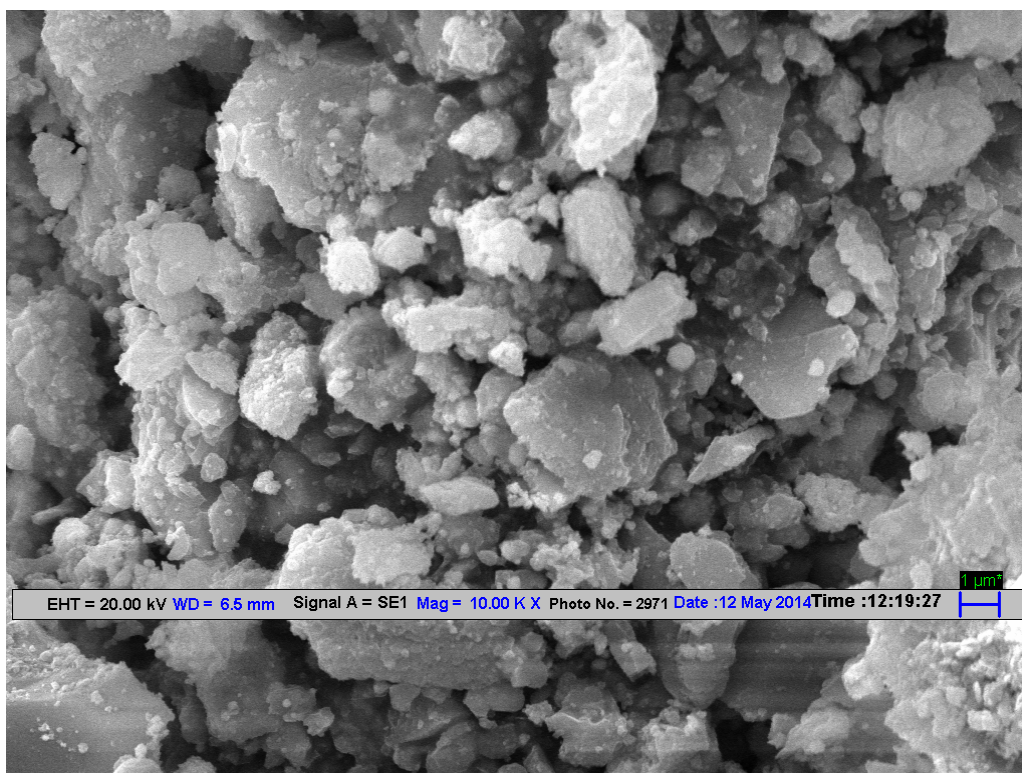


Fig. S26 SEM image of NPs after annealing obtained from **1** during Heck reaction

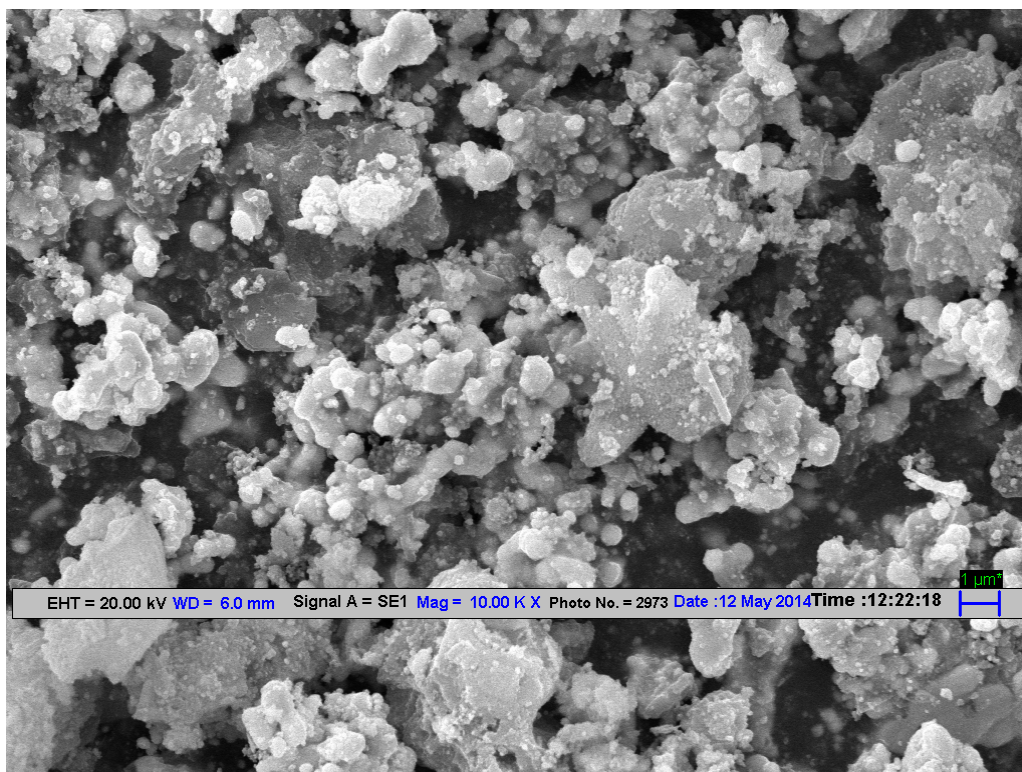
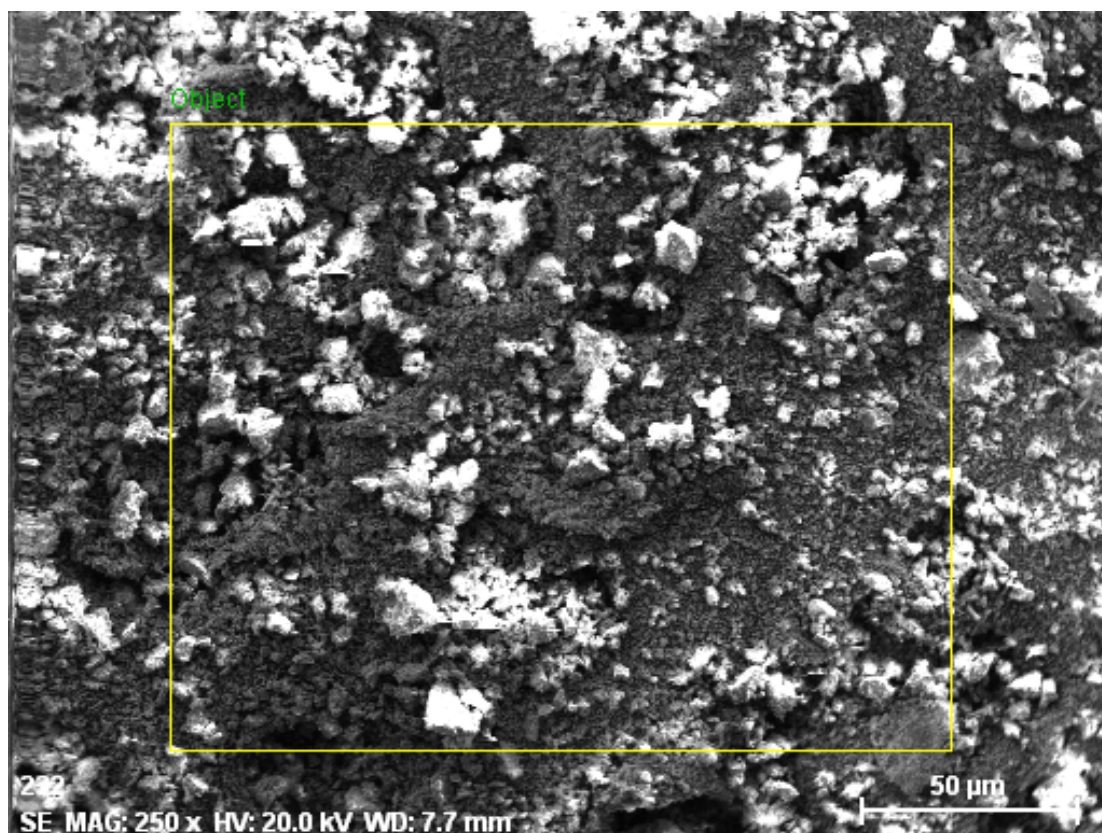


Fig. S27 SEM image of NPs after annealing obtained from **2** during Heck reaction



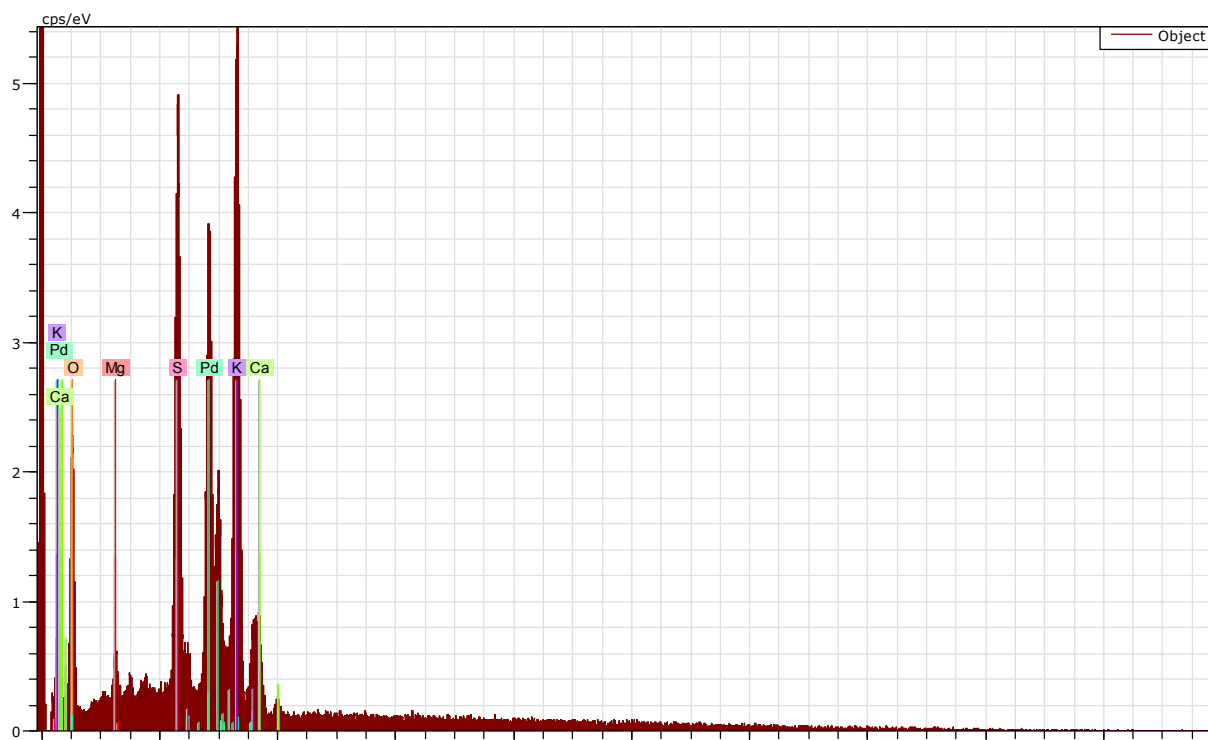
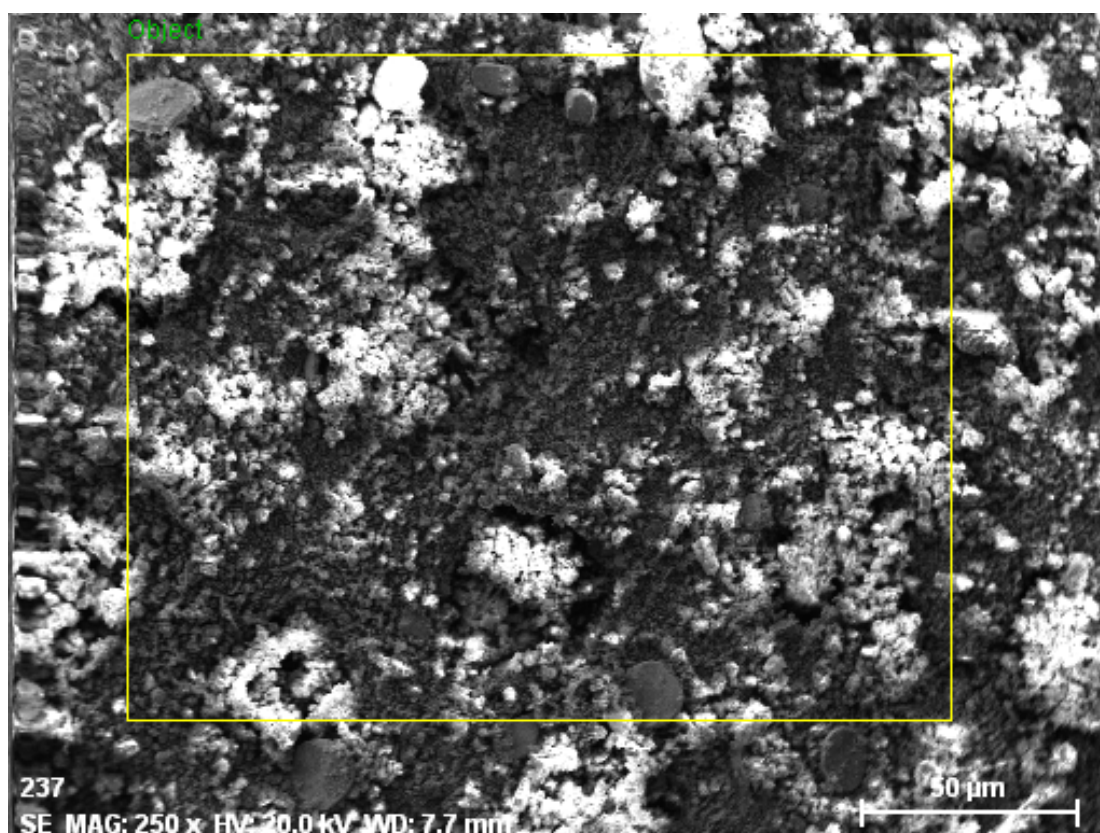


Fig. S28 SEM-EDX image of NPs after annealing obtained from **1** during Suzuki-Miyaura reaction



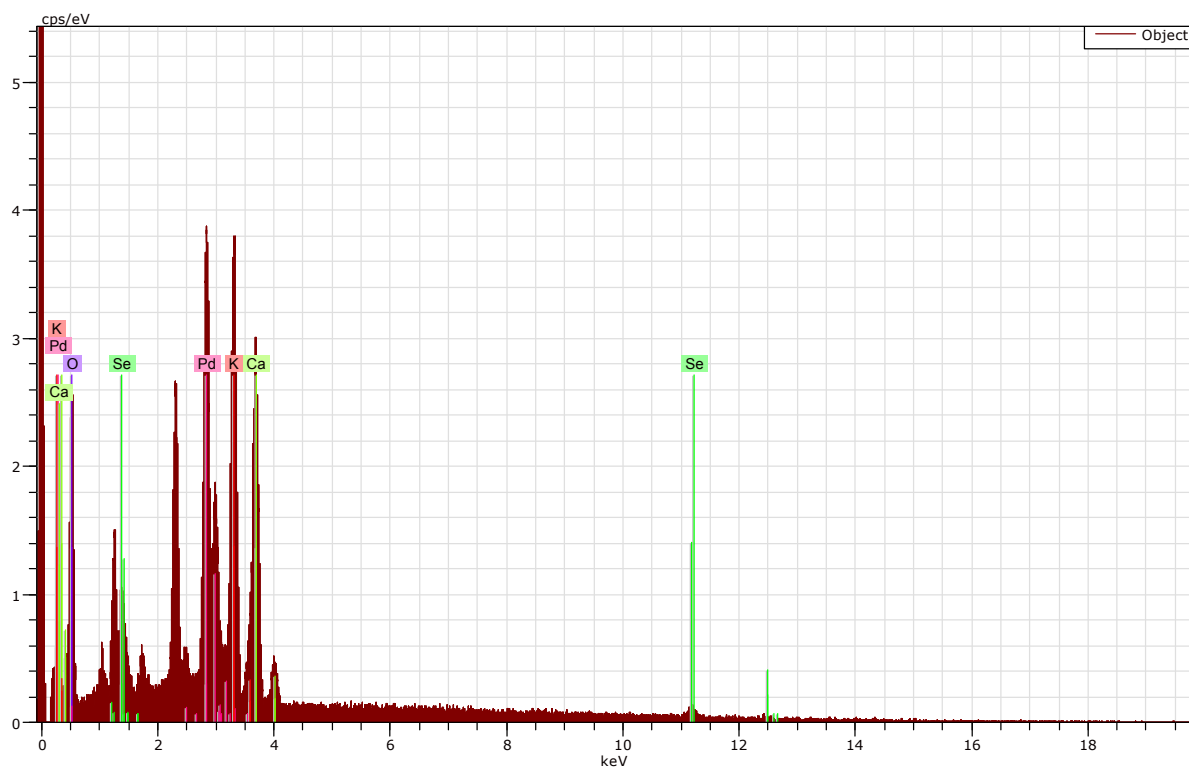
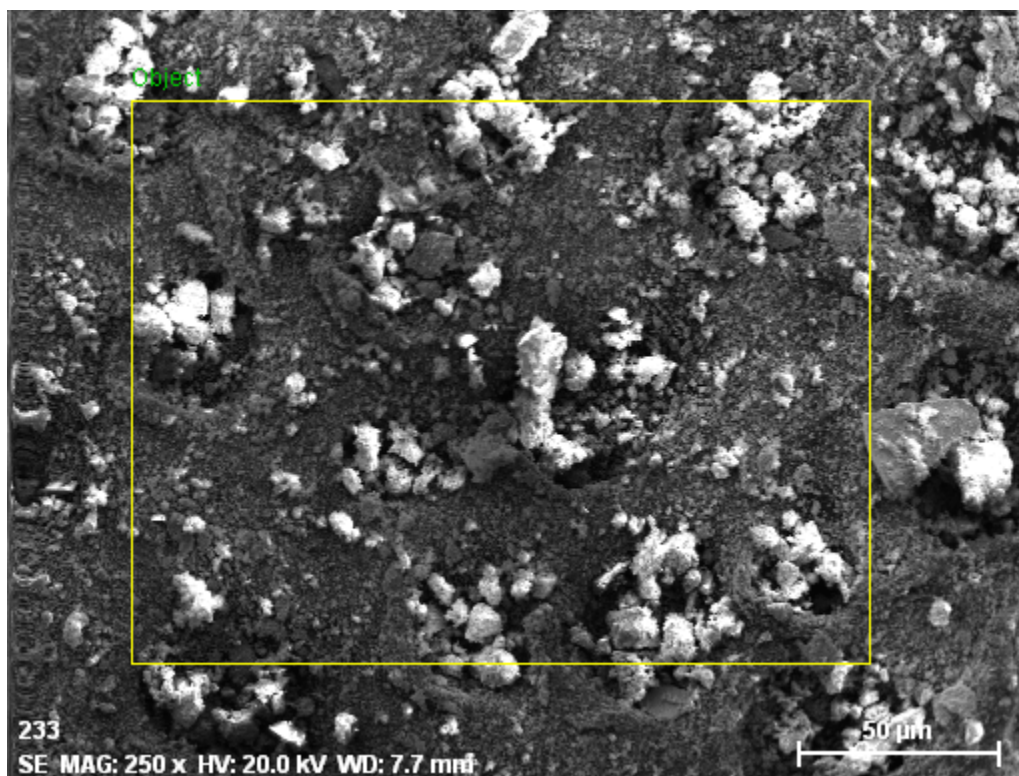


Fig. S29 SEM-EDX image of NPs after annealing obtained from **2** during Suzuki-Miyaura reaction



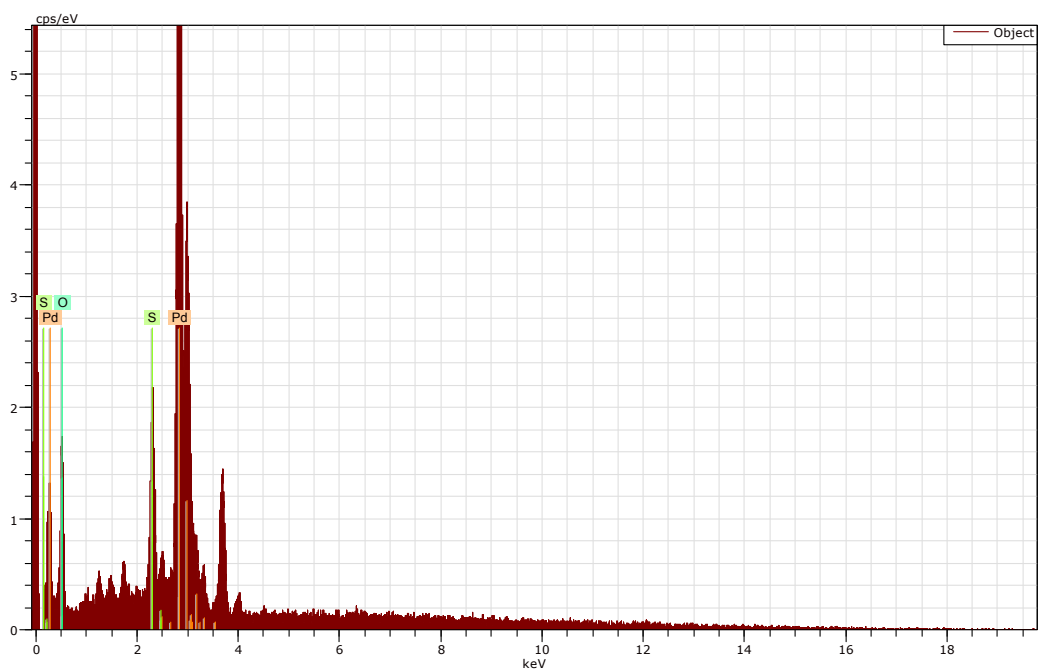
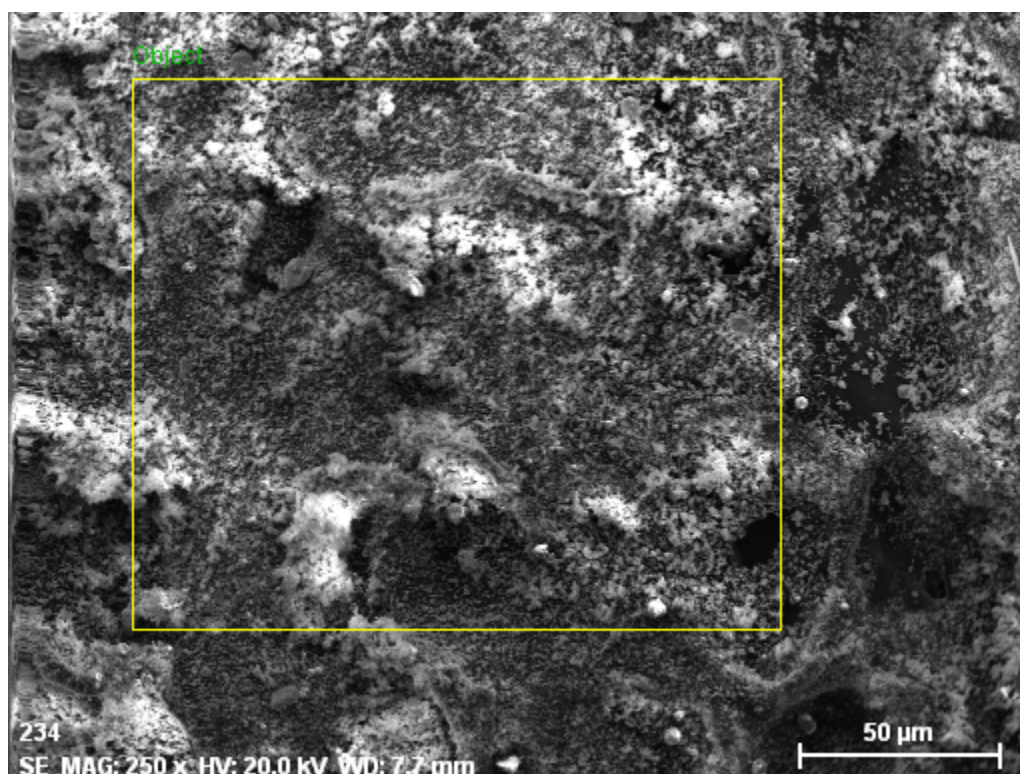


Fig. S30 SEM-EDX image of NPs after annealing obtained from **1** during Heck reaction



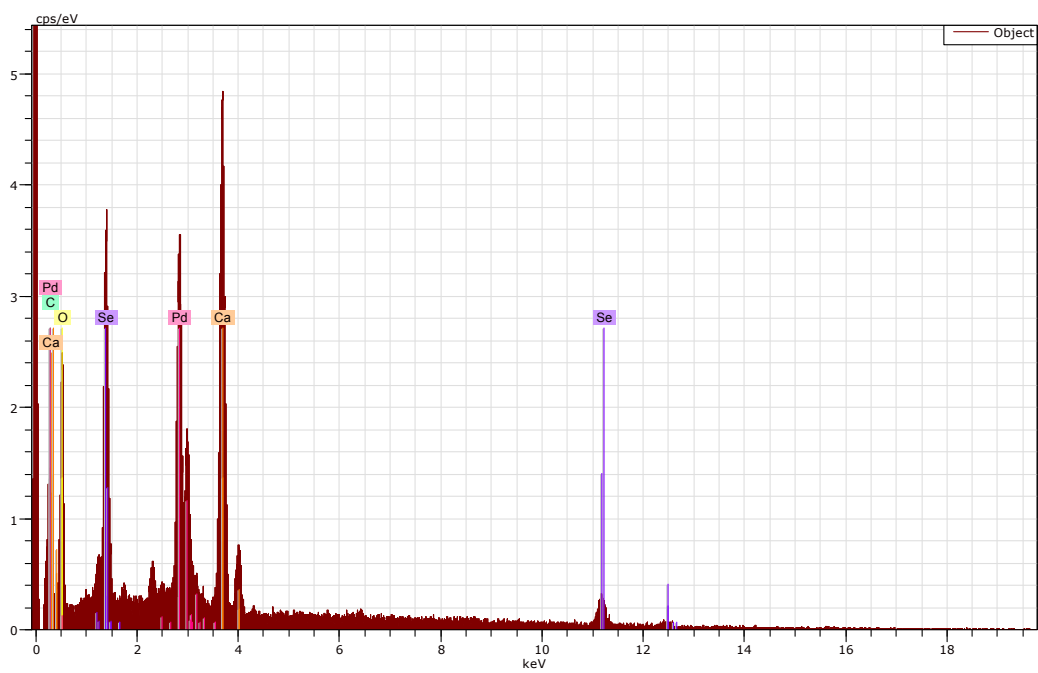


Fig. S31 SEM-EDX image of NPs after annealing obtained from **2** during Heck reaction